Towards Modeling the Complexity of the Chemical Mechanism in SERS

Imran Chaudhry,[†,‡] Gaohe Hu,[†,‡] Hepeng Ye,[†,‡] and Lasse Jensen[*,†]

†*Department of Chemistry, The Pennsylvania State University, 104 Benkovic Building, University Park, 16802, United States*

‡*Contributed equally to this work*

E-mail: jensen@chem.psu.edu

Abstract

Surface-enhanced Raman scattering (SERS) provides detailed information about binding of molecules at interfaces and their interactions with the local environment due to the large enhancement of Raman scattering. This enhancement arises from a combination of the electromagnetic mechanism (EM) and the chemical mechanism (CM). While it is commonly accepted that EM gives rise to most of the enhancement, large spectral changes originate from CM. To elucidate the rich information contained in SERS spectra about molecules at interfaces, a comprehensive understanding of the enhancement mechanisms is necessary. In this perspective, we will discuss the current understanding of the enhancement mechanisms and highlight their interplay in complex local environments. We will also discuss emerging areas where the development of computational and theoretical models are needed with specific attention given to how the CM contributes to the spectral changes. Future efforts in modeling should focus on overcoming the challenges presented in this perspective in order to capture the complexity of CM in SERS.

Introduction

One of the characteristic properties of plasmonic materials is their ability to enhance and concentrate the electromagnetic field at the surface of nanoparticles (NPs). This leads to a large enhancement of the optical properties of molecules in the vicinity of the metal surface, which can be exploited in surface-enhanced spectroscopic techniques such as surface-enhanced Raman scattering (SERS).[1–4] Since its discovery,[5–7] SERS has become a multi-disciplinary tool with applications in chemical and biological sensing[1,2,8–11] down to the single molecule limit.[12–16] SERS has also been extended to other analytic techniques such as tip-enhanced Raman scattering (TERS)[17–20] which has offered single molecule images with subnanometer resolutions.[21,22] For this reason, SERS can be used to obtain detailed information about surface chemistry of molecules at interfaces.[12,23–28]

The enhancement mechanism of SERS results from a combination of the electromagnetic mechanism (EM) from the strong near field, and the chemical mechanism (CM) from the specific interactions between the molecule and the surface.[1–4,29–33] The exact role and importance of these two mechanisms has been debated since the discovery of SERS, but it is now well accepted that the majority of the enhancement comes from the EM.[23,31,34–36] Although EM contributes the majority of the enhancement, it is the combination of the EM and the CM that leads to the observed SERS spectrum. Thus, the CM plays a crucial role in determining the relative intensities of different Raman bands and provides important information about the interactions with the local molecular environment. The CM is often expressed differently for each molecule and therefore our understanding of the CM is much less developed than the EM. For these reasons, simulations are often necessary for understanding the CM and interpreting the SERS spectra. This is particularly true as the experimental control of the local environment continues to improve, providing a more detailed view of the combined EM and CM enhancement. Therefore, an explicit treatment of the local environment becomes necessary when modeling the spectroscopy in order to fully capture the enhancement mechanisms. Ultimately, SERS provides opportunities and challenges for simulations due to

the complex interplay between the EM and the CM.

In this perspective we will highlight our current understanding of the enhancement mechanism in SERS and recent advances in modeling the spectroscopy. We will focus on current challenges, future directions and emerging areas where establishing a better understanding of the CM and developing computational and theoretical models will be necessary for advancing the field.

SERS Enhancement Mechanisms

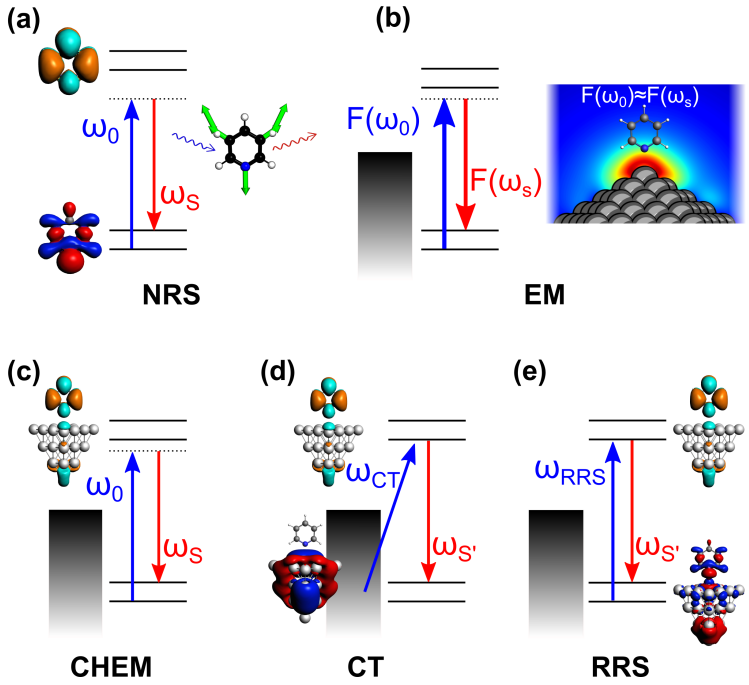

Figure 1: A diagram of normal Raman scattering (NRS) is shown in (a). Different enhancement mechanisms of SERS are illustrated: electromagnetic mechanism (EM) in (b), static chemical mechanism (CHEM) in (c), charge-transfer mechanism (CT) in (d), and resonance Raman mechanism (RRS) in (e).

The SERS enhancement mechanisms increase the Raman scattering by 6 to 12 orders of magnitude.[37–40] A majority of the enhancement is due to the EM from the strong near field generated by the plasmon excitation.[23,41–44] Compared to normal Raman scattering (NRS), the near field enhances both the incident and scattered light[33,36,43,45–47] as illustrated

in Figure 1(a) and (b). As a consequence, the EM enhancement in terms of the near-field enhancement factor F is usually approximated as $F(\omega_0)^2 \cdot F(\omega_s)^2$, which can be simplified as $F(\omega_0)^4$ if the difference in incident and scattered light is small.[33,36,48] The description of the EM enhancement in terms of the near field assumes that the field is homogeneous over the dimension of the molecule. For NPs with atomistic protrusion, studies have shown that field gradient effects become important and thus additional enhancement mechanisms due to inhomogeneous near field need to be considered.[44,49–54] For metallic SERS substrates, the EM has been shown to give an enhancement factor on the order of 4 to 10 orders of magnitude.[48,55–58] Because the EM arises from the plasmon resonance, it is typically assumed to be independent of the electronic structure of the molecule adsorbed on the surface.[32–34,36]

Unlike the EM, the CM is directly related to the electronic structure of the molecule on the surface. Understanding the CM requires accounting for the wave function overlap of the molecule and the surface leading to the renormalization of the molecular energy levels alongside the introduction of metal-molecule charge-transfer states. In this way, the CM can be categorized in terms of three distinct contributions: static chemical interactions (CHEM), charge-transfer resonance (CT), and molecular resonance Raman scattering (RRS).[31,33,59–61]

CHEM is a consequence of renormalizing the molecular energy levels leading to the decrease of the energy gap of the molecule, as shown in Figure 1(c). This decrease in energy gap results in an overall increase in the polarizability of the molecule,[62] thereby increasing the Raman scattering and leading to the CHEM enhancement. In addition, the changes in the geometry and electronic structure of the molecule on the surface lead to shifts in the vibrational frequencies. These changes are significant enough to affect the Raman scattering and are included in the CHEM contribution.[32,63–66] Since the CHEM contribution does not involve processes that are resonant with the incident light, it is relatively weak with an enhancement factor of around 1 to 2 orders of magnitude.[61,62,65,67–70]

Much larger SERS enhancements can be observed when the energy of the incident light is resonant with an electronic transition. Such electronic transitions can either involve ex-

citations between the metal and the molecule, or remain localized to the molecule.[71,72] The former excitations lead to the CT contribution, which is illustrated in Figure 1(d). Charge-transfer processes involve metal-molecule states and are usually weak and hard to detect, thereby making it difficult to quantify its enhancement. The other excitations lead to RRS, which is illustrated in Figure 1(e). Although RRS is not limited to SERS, it is different due to the molecular electronic and geometric changes from binding to the surface. Also, RRS detection without the substrate is hindered by the presence of strong fluorescence.[73,74] In contrast, metal surfaces quench the fluorescence, thereby making surface-enhanced resonance Raman spectroscopy (SERRS) possible.[75] These on-resonance contributions can lead to large enhancement factors with about 2 to 4 orders of magnitude from CT[76,77] and about 4 to 6 orders of magnitude from RRS.[74] For this reason, single molecule SERS is often performed under resonance condition due to the large enhancement.[13,14,24,37]

Even though the EM is the dominant mechanism, describing the CM is critical for fully interpreting SERS spectra and can lead to key insights about the electronic structure and geometry of the molecule on the surface. The main obstacle in correctly identifying either of the mechanisms is the fact that they contribute collectively to the overall enhancement, leading to difficulties in quantifying them in both experiment and theory. Traditionally SERS is done on metallic substrates, but recently more diverse substrates have been introduced involving non-plasmonic substrates where the CM gives the dominant contribution. Furthermore, SERS is increasingly being used to track dynamic behaviors of molecules, chemical reactions, and electrochemical events at the interfaces even at the single molecule level. Additionally, the control of the local environment in TERS has enabled Raman imaging of individual vibrations thus pushing Raman scattering into sub-molecular level. Taken together, this reflects the multitude of complex local environments that needs to be considered when modeling SERS. Therefore, it is increasingly important to accurately describe the CM and its interplay with the EM.

Approaches to Separating the EM and the CM

It is important to understand the relative intensities of the molecular vibrational changes when bound to the surface to extract the rich chemical information from SERS experiments.[23,51,60,78–80] If the EM and the CM can be separated, interpretation of SERS spectrum can be made easier. For example, a detailed understanding of the CM can inform us about the specific interactions between the molecule of interest and the surface,[23,31,32] while a detailed understanding of the EM can provide us with information about the orientation of the molecule on the surface.[36,51,81,82] However, a clear-cut distinction between these two mechanisms is not possible.[59,68–70,83] Therefore, the interpretation of the spectrum will reflect how the coupling between the two mechanisms are treated.

If the CM is ignored, relative intensity changes can be attributed to molecular orientations changes relative to the near field which is known as the SERS surface selection rules.[36,84–86] These rules dictate that the molecular normal modes aligned with the local field will have the largest enhancement, and enable molecular orientation to be determined by comparing experimental and theoretical Raman spectra.[82,84,87–93] In most cases, the theoretical Raman spectrum is obtained for either a free molecule that is oriented in different ways along the near field axis or a molecule adapting different configurations on small nanoclusters.[93–97] In this way, the CM is assumed to be either minimal or captured in the simulation of the molecule on the nanocluster and the coupling between the EM and the CM is neglected. Furthermore, it is likely that many configurations contribute to the overall SERS spectrum.[93,98,99] For example, it has been shown that both flat and vertical molecular configurations can simultaneously be detected with SERS even if the flat configuration is energetically more favored.[93] For this reason, the determined orientation is best considered as a representative of the average geometry of the molecule. In addition, the surface selection rules assume that the near field does not vary over the length-scale of the molecule. While it is generally true, studies have shown that for atomic-scale roughness, variation of the near field over the dimension of the molecule becomes important.[100–102] Significant near field gradients lead to

the enhancement of normally non-Raman active modes as well as changes to the relative peak intensities.[98,103–107] These changes can be described by a set of field gradient surface selection rules that incorporate additional scattering mechanisms such as dipole-quadrupole and quadrupole-quadrupole scattering not observed in NRS.[51–53,107,108] As a consequence, more information about molecular orientation can be extracted when near field gradient effects are large. Finally, it has been demonstrated that SERRS cannot determine molecular orientation when on-resonance with a single molecular state.[109] For these cases, non-linear spectroscopy such as surface-enhanced hyper-Raman scattering (SEHRS) offers additional information about molecular orientation through the non-Condon effect.[109,110]

A few different experimental approaches have been proposed to extract the CM. One approach to estimate the CM is to correct relative experimental SERS intensities by estimated EM enhancement.[69] This assumes that the CM is frequency-independent and the near-field enhancement mirrors the frequency-dependent extinction spectrum. Another way to determine the relative CM enhancement is to normalize the spectra with respect to a mode that is predominantly enhanced by the EM.[68] The assumption is that the EM is the same for all vibrations, which is expected if the plasmon is broad and the vibrations are close in frequency to the mode used in the normalization. Alternatively, an approach to compare relative enhancement between molecules has also been proposed.[70] This approach relies on substrates with highly uniform EM enhancement over a large area such that the variation of enhancement factors can be attributed to the CM. This assumes that the EM is independent of the molecule and that molecules have similar orientations and binding affinities with the surface. The estimations of the CM in these ways have been shown to be in good agreement with electronic structure calculations. In general, these approaches neglect the coupling between the EM and CM and cannot be easily generalized to on-resonance cases. Another way to study the CM is to use non-plasmonic substrates, which will be discussed in the following section.

Efforts have been made to characterize charge-transfer contributions to SERS. One ap-

proach to characterize CT mechanism is to vary an applied potential such that any charge-transfer excitations can go on- and off-resonance.[111,112] Modes that have large CT contribution will have large intensity changes which can be used to quantify CT enhancement for each vibration. This approach considers all contributions to be from CT, while other aspects such as molecular reorientation, changes to the molecular structure, or changes to the substrate can also contribute to relative intensity changes.[94,113,114]

Since the EM dominates the enhancement mechanisms, many theoretical studies focus on quantifying the near field enhancement. The near field from large NPs is typically well approximated using classical electrodynamics.[115–118] To treat electronic structure of the molecule, hybrid methods that combine a classical electrodynamic description of the NP with a quantum mechanical description of the molecule have been developed.[100,119–125] These hybrid methods can incorporate the site-specific atomistic near field and have been shown to give good description of the EM and naturally incorporate field gradient effects.[100,123–125] However, these hybrid models do not fully describe interaction between the molecule and the substrate such as charge-flow and thus CM is not included. In contrast, full quantum mechanical methods treat all enhancement mechanisms at the same level,[126–131] and thus it remains a challenge to interpret individual enhancement mechanisms.

One possible interpretation scheme is based on the analysis of selected electronic transitions within and between the substrate and the molecule. An example of a transition-based scheme is the unified view of SERS model in which the interplay between enhancement mechanisms can be identified based on the involved transitions and their resonance nature.[71,72] The unified view of SERS shows how different mechanisms contribute to the overall enhancement and is commonly used to interpret the charge-transfer enhancement of SERS.[132–134] Another example utilizing transition-based scheme is a simplified two-state model where a quantitative relationship between the CHEM enhancement factor and the alignment of molecular orbitals and the Fermi level of the substrate can be established.[61,62] The two-state model has been shown to give good agreement with full quantum mechanical and experimen-

tal estimations of the CHEM enhancement factors. Another possible scheme is to interpret enhancement mechanisms based on charge-flow in the molecule-substrate complex, such as Raman Bond Model (RBM).[63,83,135] In this model, the total Raman intensities are partitioned into atomic and interatomic contributions, with the latter referred to as the Raman bonds. Based on this partitioning, the RRS, EM and CT enhancements can be identified as Raman bonds within the molecule, the substrate and between the substrate and the molecule, respectively. The interplay between the CT and EM enhancement mechanisms and consequently the difficulty in separating the mechanisms are highlighted in RBM.[135] In general, the RBM enables quantitative analysis of different enhancement mechanisms and avoids the consideration of only a few selected electronic transitions.

As discussed above, the full description of SERS requires the full incorporation of the CM and the EM which naturally necessitates the use of full quantum mechanical methods. The major challenge for full quantum mechanical methods is the ability to carry out calculations for NPs that are large enough to support plasmonic excitations. Therefore efficient methods are needed such as simplified quantum mechanical methods or hybrid models that allows for the CM and the EM to be treated simultaneously. Further development in interpreting the full quantum mechanical results are needed, especially regarding the interplay between the EM and CT.

SERS from Non-Plasmonic Substrates

Plasmonic substrates are primarily used in SERS due to the large EM enhancement which makes it difficult to study the CM enhancement. Alternatively, using non-plasmonic substrates can effectively eliminate the EM, thereby leaving only the CM.[77,136–138] Organic semiconductors,[139,140] metal-organic frameworks (MOFs),[141,142] perovskite nanocrystals,[143,144] copper telluride nanoparticles[145] and also 2D materials, such as transition metal dichalcogenides[146–149] along with graphene[146,150–152] and its derivatives,[153] have emerged as SERS

substrates. The variety of these non-plasmonic SERS substrates provides an experimental platform for studying CM. Although there are no plasmon resonances in these types of substrates, Mie resonances in large nanostructures can give significantly enhanced Raman signal through EM.[154,155] For simplicity, here we will focus on understanding the CM. The full understanding of the CM could lead to rational design of non-plasmonic SERS substrates that are tailored to sense specific molecules.

For non-plasmonic substrates, the CT mechanism is often invoked to explain the enhancement. This is due to the emergence of charge-transfer excitations in the interface between molecules and non-plasmonic substrates.[76,147,156] For example, in semiconductor substrates, charge-transfer excitations from substrate valence band (VB) to molecular LUMO or from molecular HOMO to substrate conduction band (CB) arise.[138,157] The CT enhancement is determined by the molecular orbital (MO) alignment relative to the substrate energy band[157–159] and can be tuned by controlling their relative alignment. Consequently, the optimal energy level alignment to achieve large enhancement is that the energy difference is in resonance with the incident light. The study of CT mechanism can be done by tuning incident light frequency to be resonant with the charge-transfer excitations.[76,160] The charge-transfer excitations responsible for the enhancement has in some cases been identified by differential absorption, thereby providing direct evidence of CT mechanism.[76,147,156] The CT enhancement of these substrates is usually reported to be less than 10^4,[146,149] but larger enhancement has also been achieved.[161,162] The advantage of non-plasmonic substrates is their greater tunability of the enhancement at the expense of less enhancement compared to metallic substrates. For example, tuning of the CT mechanism can be achieved by changing molecule functional groups,[163,164] modifying substrate energy bands through chemical doping,[151,153,165,166] electrochemical gating,[151,167] or simply changing the substrate.[146,168] Beyond the CT mechanism, RRS-like enhancement is also possible when the incident light is on resonance with an electronic transition in the substrate.[157,169] Larger enhancement due to synergistic effects can be achieved by aligning the transitions within the substrates either

with the transitions in the molecule[170,171] or with the CT transitions.[172–175] Similarly, it has been shown that the excitations can be combined with Mie resonances to generate larger enhancement.[176–178] Furthermore, it has been shown that the CM is also dependent on the molecular orientation.[179,180] For example, on graphene surface, the lying-down configuration of the planar molecule can lead to larger enhancement due to larger chemical interactions with the surface.[180]

Compared to simulations for plasmonic substrates, much less work has been done on modeling SERS for non-plasmonic substrates. Modeling CT mechanism for non-plasmonic substrates requires careful consideration of both the geometry of the substrate and the binding geometry of the molecule since charge-transfer excitations depend strongly on these factors.[181] The two-state model has also been generalized to explain CHEM enhancement on non-plasmonic substrates.[67,182] Using this model, it has been shown that tuning an external potential can modulate the CHEM enhancement mechanism by aligning the molecular LUMO with respect to the VB.[182] Another result of the model for a graphene substrate is that electron-phonon coupling can lead to damping of the Raman intensity of adsorbed molecules.[67] This indicates that although narrowed energy gap can in general lead to larger enhancement, an optimal energy level gap is needed to balance between the CHEM enhancement and the damping mechanisms.

To further understand the CM from non-plasmonic substrates, advances in theoretical methods dedicated to charge-transfer excitations are needed. This is because charge-transfer excitations are generally difficult to model with electronic structure theory.[183–185] As discussed above, other electronic transitions and coupling between these transitions can lead to larger enhancement than expected from the individual mechanisms. While this has been achieved experimentally, theoretical calculations addressing synergistic effects in the coupled enhancement mechanisms are required to gain further insights and understanding.

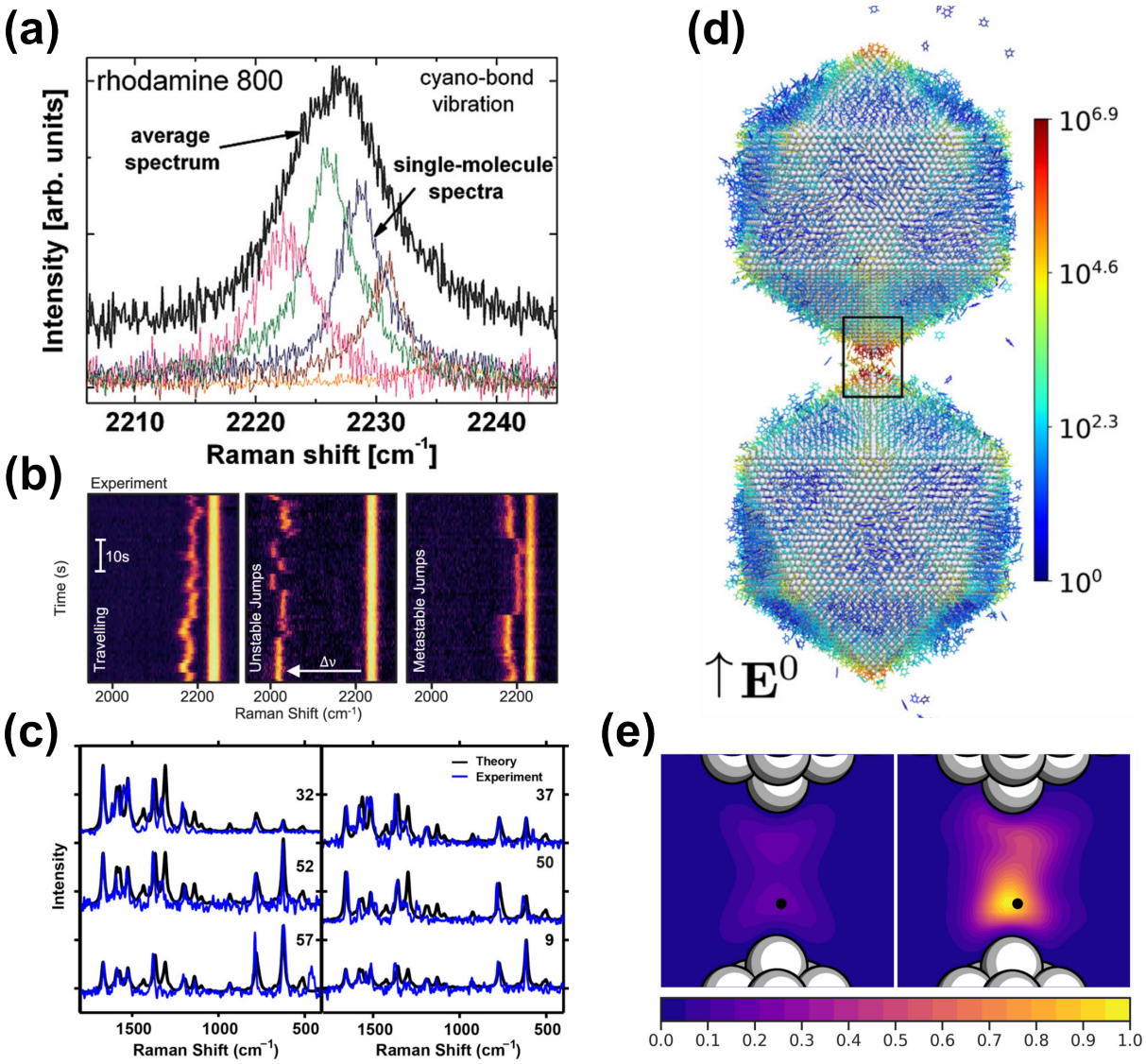

Figure 2: (a) Comparison between average and single-molecule spectra of rhodamine 800. Adapted with permission from ref. 186. Copyright 2010 American Chemical Society. (b) Time trajectory of single CN stretching mode. Adapted with permission under a Creative Commons CC BY License from ref. 187. Copyright 2021 Springer Nature. (c) Single-molecule experimental and theoretical TERS spectra due to excited state fluctuations. Reprinted with permission from ref. 188. Copyright 2013 American Chemical Society. (d) Illustration of enhancement factor distribution in a large dimer system. Adapted with permission from ref. 98. Copyright 2016 American Chemical Society. (e) Comparison of electric field distribution in a silver junction with (right) and without (left) solvent. Adapted with permission from ref. 100. Copyright 2021 AIP Publishing.

Strong enhancement from localized hotspots allows detection of Raman signal from in-

dividual molecules.[13,14,24,26,37,189,190] Single-molecule SERS (SM-SERS) depends strongly on the local environment of the molecule and can be used as a reporter of the dynamics of the molecule on the surface.[186–188] In contrast to SM-SERS, most experiment are done under conditions where many molecules contribute to the signal. The resulting spectra reflect the different orientations and local environments of the molecules.[26,37,189,191,192] An example of this is illustrated in Figure 2 (a) where a series of single-molecule spectra is shown to be distinct from the average spectrum. Often a small fraction of molecules with specific orientations dominates the signal, therefore modeling focuses on capturing their local environments.[93,94] Generally, models should account for different molecular orientations and their interactions with the substrate as well as the solvent and ligand effects. However, this is rarely done due to the high computational costs from averaging over these degrees of freedom to model ensemble-averaged SERS (EA-SERS).[98] Describing SM-SERS and EA-SERS poses challenges for theory, but offers the potential to gain more detailed insights into the molecule-surface interactions through modeling the CM.

SM-SERS requires large EM enhancement from spatially localized hotspots[26,37,189,190] often combined with strong CM enhancement from RRS,[14,192–194] although it has been shown that under non-resonant conditions it is still possible to detect SM-SERS signal.[192,195] Another possible approach to achieving single molecule detection with Raman is through TERS (SM-TERS) that makes use of gaps between plasmonic tips and substrates to gain spatial resolution and localized hotspots.[22,103,196,197] In SM-SERS and SM-TERS, there are dynamic changes to both spectral positions and intensities due to, for example, the diffusion of the molecule in and out of the localized hotspots and reorientation inside the hotspots.[24,187,198–201] The dynamics of the molecule samples different enhanced near field which affects the Raman scattering. One example is shown in Figure 2 (b), where the dynamical changes of a CN stretching mode in SM-SERS are monitored to track the thermal diffusion of a metal adatom. In this setup, the hotspot was created by an adatom and computational modeling was used to map the dynamical changes in the SERS spectra to the dynamics of the adatom, hinting

at the possibility of extracting chemical dynamics from SM-SERS. Furthermore, the fluctuations due to rotational dynamics of the molecule in the hotspot can in principle be used to track the molecular orientations,[88,202] especially if field gradient effects are important. Another possible origin of fluctuations in SM-SERS can be related to the RRS mechanism where subtle changes in excited state properties can lead to drastic changes in the Raman spectra. This is shown in Figure 2 (c) where drastic changes in the TERS spectra are observed.[188] Computational modeling shows that these fluctuations can be explained by minute changes to the excited state geometry, although the origin of the geometric changes were not identified. This suggests that the excited state properties can be extracted from the dynamic changes in SM-SERS and SM-TERS. Finally, it has been shown that non-equilibrium excited state manifold influence CHEM and therefore the SM-SERS spectra.[203]

Even when not in the single-molecule limit, only a small fraction of molecules contribute the majority of the signal due to the small surface area of the hotspots. For example, it has been demonstrated that about 5% of the molecules on the surface contribute about 85% of the signal.[55,98,204] This is due to the EM being strongest in the junctions and crevices between NPs, which constitutes a small region of the surface. This is illustrated in Figure 2 (d), where the Raman enhancement of molecules coating a silver dimer is shown. Each molecule is color coded according to its enhancement factor and shows that the enhancement distribution is dominated by the few molecules sitting in the junction. Explicit modeling of EA-SERS has been performed by averaging over millions of SERS spectra from sampled configurations of NP fully coated with molecules. By calculating the Raman scattering of every molecule on the NP, the simulation detailed how the specific locations and orientations of adsorbed molecules, as well as the near field gradient, contribute to the overall spectra.[98] However, only the EM was considered and the interactions between the molecules were neglected.

Beyond molecules in a hotspot, the influence of solvent/ligand interactions should also be considered when modeling SERS.[100,205] For solvent effects, this is typically done using hybrid methods that either treat the surrounding using a continuum model[122,206–208] or an explicit

classical model.[100,209] The presence of solvent/ligand interactions strongly affects the near field distribution around NPs.[100,118,210] An example of this is illustrated in Figure 2 (e), where the electric field distribution is symmetric without solvent molecules but becomes asymmetric with solvent molecules present. Furthermore, the change of the spatial distribution of the near field increases the field gradient in the gap. The enhancement factor due to solvent effects has been shown to be of the same magnitude as the CM[100] and thus should be considered when modeling SERS.

Similarly, it has also been shown that ligands perturb the near field.[210–212] For example, halide ligands are known to induce aggregation of NPs[213,214] and consequently control the formation of hotspots determining the EM enhancement.[215–217] In addition, the SERS enhancement can be affected by the modified binding affinity of the molecule,[216,218–220] as well as desorption of the molecules from the surface[221,222] due to the presence of halide ligands. Halide ligands can also tune the Fermi level of the substrate which changes the interactions between the molecule and the substrate.[223,224] It has been shown that the binding of halide ions can change the interfacial structure and active binding sites, leading to molecular reorientation.[225] This also leads to changes in the frontier orbitals, which results in a stronger CHEM as well as modulation of charge-transfer excitations contributing to the CT.

Challenges remain in resolving chemical information in SERS originating from molecule-substrate interactions due to diffusion, orientation, field gradient effects and solvent/ligand effects. The need to model these effects will necessitate the use of quantum mechanical models combined with sampling over many degrees of freedom leading to high computational costs. To overcome these challenges, it will be necessary to develop multiscale models that describe both the EM and CM, while also being efficient enough to allow sampling. This will be key to understand the interplay between the enhancement mechanisms in these complex local environments.

SERS in Electrochemical Environments

Electrochemical SERS (EC-SERS) enables *in situ* investigation of absorption and chemical changes at electrodes.[226–230] It has been shown that under resonant conditions, single-molecule EC-SERS is possible,[24,231] thus enabling the monitoring of electrochemical events at the single-molecule level.[231] Under electrochemical conditions, the applied potential gives rise to changes in relative intensities as well as band shifts. One reason for these changes is the modulation of the Fermi level by the applied potential which consequently affects the charge-transfer process.[114,128,232] Furthermore, the applied potential affects the local electric field at the surface and vibrational frequencies will shift due to the Stark effects.[233–235] Here the local electric field refers to both the interfacial field in the double layer and the plasmonic near field that gives rise to the enhancement. Additionally, spectral changes due to the applied potential may also be related to reorientation of the molecule.[51,236–239] In general, information about interactions between the molecule and electrode can be extracted from EC-SERS.

Relative SERS intensities have been shown to depend strongly on the applied potential which is typically explained by the CT mechanism.[114,226,240–245] There are several approaches for modeling the applied external potential using first principle methods, through incorporating an external electric field,[128,232,246,247] a charged cluster model,[112,114,242] or a modified semi-empirical approach.[245,248] Most efforts focus on modeling the bare molecule-substrate interfaces,[112,114,128,232,242,246,247] while the inclusion of electrolyte interactions in simulation is rare.[249] It has been demonstrated that an applied potential can enhance the intensity due to stronger binding, leading to an increased CT enhancement.[128,232] Experiment combined with first principle calculations has further shown that the applied potential needed to tune the CT resonances is determined by the electron affinity of the molecule.[243] This can also be used to explain the observation that SERS spectra under CT resonance conditions resembles NRS spectra of the molecular anions.[243,250,251] In addition, calculations of CT enhanced spectra have shown that vibrational modes are preferentially enhanced when the MOs as-

sociated with the charge-transfer excitations are localized at the vibrating atoms.[243,252,253] While CT is often invoked to explain the dependency of SERS on the applied potential, electric field changes, reorientation, and redox processes should also be considered when explaining relative intensity changes in EC-SERS. EC-SERS can be used to determine the electric field in the interfacial double layer due to the shifts of vibrational bands through the Stark effect.[234,235,254–256] The resulting changes in the interfacial electric field can lead to reorientation of the molecule such that certain modes can be selectively enhanced due to the surface selection rules.[89,257] In addition, the applied potential can induce redox reactions at the interface that lead to significant changes to the spectra.[94,230,231,236] Since changes to the interfacial electric field, orientation, and CT mechanism are induced simultaneously by the applied potential, the potential dependence in EC-SERS is complicated and all effects must be considered to correctly interpret the relative intensity changes.

In general, the applied potential is mainly thought to influence CM in SERS. However, it has been shown that the applied potential can directly influence the EM.[135] To fully account for the EM, the influence of the applied potential on the electronic structure of the substrate should be considered due to the coupling with the CM mechanism. Furthermore, to understand and exploit the full potential of EC-SERS, a better connection between theoretical calculations and experimental observations are needed. Especially possible ways of separating the contributions of CT mechanism and reorientation of the molecules are needed to extract the rich information about molecular behaviors at surfaces.

TERS for molecular imaging

The main advantage of TERS is the combination of SERS and scanning probe microscopy (SPM) where the confined electromagnetic field in the junction leads to enhanced Raman scattering.[26,258–261] As a consequence, Raman signal in TERS is sensitive to tip positions[104,262–265] and it is possible to visualize individual vibrational modes of a single molecule

by its TERS image.[22,197,199,266,267] The confined near field also introduces significant field gradient effects that lead to modified selection rules compared to regular SERS.[24,103,107,268–271] Because of the high sensitivity and spatial resolution of TERS, the environment of a single molecule can be precisely determined which makes it a controllable platform for exploring Raman enhancement mechanisms.

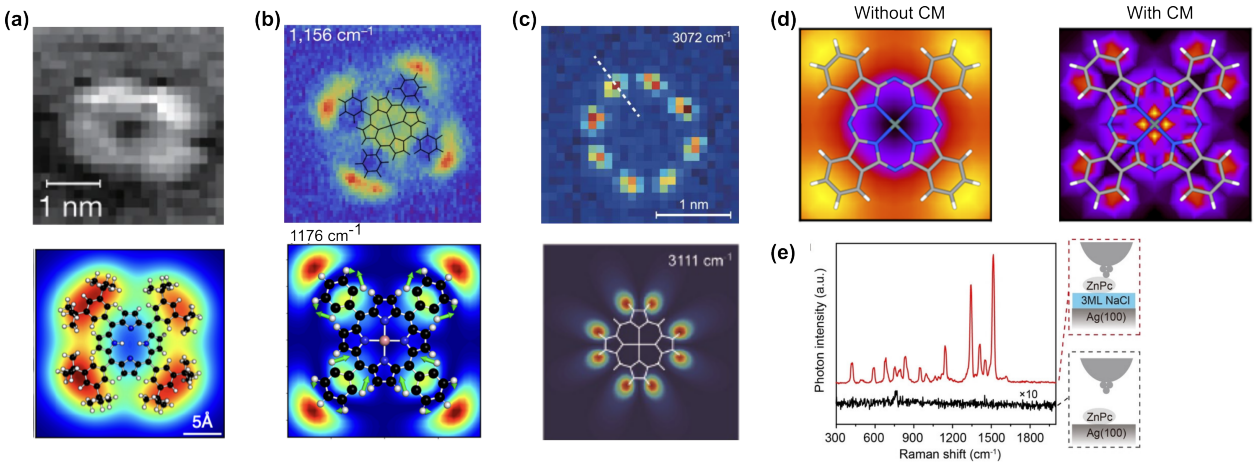

Figure 3: (a) Top: TERS image of H_2TBPP molecule on Ag(111). Adapted with permission from ref. 22. Copyright 2013 Springer Nature. Bottom: Simulated TERS image of H_2TBPP molecule on Ag. Adapted with permission under a Creative Commons CC BY License from ref. 104. Copyright 2019 Springer Nature. (b) Top: TERS image of a vibrational normal mode of CoTPP molecule on Cu(100). Adapted with permission from ref. 21. Copyright 2019 Springer Nature. Bottom: Simulated TERS image of a vibrational normal mode of CoTPP molecule on Cu. Adapted with permission from ref. 103. Copyright 2019 American Chemical Society. (c) Top: TERS image of a vibrational normal mode of Mg-porphine on Ag(100). Bottom: Simulated TERS image of a vibrational normal mode of Mg-porphine on Ag. Adapted with permission under a Creative Commons CC BY License from ref. 272. Copyright 2019 Oxford University Press. (d) Simulated TERS image of SnPc with (right) and without (left) CM. Adapted with permission under a Creative Commons CC BY License from ref. 273 Copyright 2023 American Chemical Society. (e) Comparison of TERS intensity of ZnPc on Ag(100) substrate with and without NaCl monolayer. Adapted with permission from ref. 274. Copyright 2023 Wiley-VCH GmbH.

Visualization of individual vibrational mode of a single molecule has been achieved by integrating the Raman signal of the frequency band, as shown in Figure 3. TERS images of a single molecule was first achieved for H_2TBPP molecule illustrated at the top of Figure 3(a) where resolution of $\sim$ 1 nm was demonstrated.[22] The spatial resolution has since been pushed to the Ångström-scale such that individual vibrational modes can be visualized as shown

at the top of Figures 3 (b) and (c) .[21,272] Because the high resolution of TERS is normally attributed to the confined near field, theoretical modeling of TERS imaging has focused on simulating the confined electromagnetic field effects.[103,104,271,272] Several different hybrid classical electrodynamic/quantum mechanical approaches have been applied to simulation of TERS images.[103,104,271,272,275] Simulations that incorporate EM[103,271,272] are shown at the bottom of Figures 3(a)-(c) for each experimental result, respectively. The generally good agreement between theory and experiment indicates that the highly localized field due to the atomic protrusions is responsible for the sub-molecular resolution. As shown at the bottom of Figure 3 (b), the field gradient effects are important in achieving the resolution, leading to bright spots that are located away from the vibrating atoms.[103] Modeling has also shown that TERS images can be explained by the sub-molecular density changes induced by the confined near field during the Raman process.[104] This also explains the breakdown of the traditional selection rules observed in high-resolution TERS.[103,104] Furthermore, it has been shown that for localized vibrations it is possible to visualize in-phase and out-of-phase motion of single chemical bond.[272] While good agreement was achieved, these simulations neglected the CM contributions to TERS. To describe CM in TERS simulations, several quantum mechanical models have been proposed.[273,276–278] An example is shown in Figure 3 (d), where a model approximating the tip by a single Ag atom was utilized.[273] Comparing to the TERS image generated by including only EM (Figure 3 (d), left), incorporation of CM (Figure 3 (d), right) leads to both increased Raman scattering as well as higher resolution. This shows that besides the EM, the CM is likely important in determining the high resolution in TERS imaging and can lead to more concentrated signals around vibrating atoms. Another contribution from the CM to single molecule TERS has been identified by comparing TERS signal with and without NaCl spacer monolayers as shown in Figure 3 (e).[274] The TERS signal without the spacer layer was found to be significantly quenched due to the direct contact of the molecule with the metal substrate. This quenching of the TERS signal was proposed to arise from the CHEM leading to screening of the Raman polarizability

caused by orbital hybridization between the molecule and metal substrate. This is contrary to the common understanding of CM that it will enhance Raman scattering.

The quenching of near field has been observed for narrowly gapped plasmonic dimer systems[279–281] due to quantum tunneling of electrons across the junction.[281–285] The reduction of the near field is expected from the EM to lead to a smaller enhancement of the Raman scattering. For example, in SERS, this reduction of the Raman enhancement for molecules in NP junctions with small separations has been observed.[281,286,287] However, TERS imaging is enabled by the strong enhancement for small tip substrate separations where quantum tunneling is expected to be important.[21] Moreover, there have also been observations of drastic enhancement of TERS signal when direct atomic contact between the tip and sample is made.[288–290] To consider quantum tunneling effects, it is required to go beyond classical electrodynamics to elucidate the complexity of narrowly gapped plasmonic systems.[285,291–293]

To fully describe TERS imaging, it is important to incorporate enhancement mechanisms beyond the EM through quantum mechanical modeling.[276,277,294] To address realistic systems, more efficient quantum mechanical methods are needed to make the calculations affordable and treat the combined effects of the CM and EM. This is important as TERS offers the potential to unravel the CM due to its sub-molecular resolution.

Outlook

The sensitivity and selectivity of SERS is the result of the large enhancement of the Raman scattering of molecule at interfaces. Although the debate over the origin of the enhancement has mostly been settled, it remains difficult both experimentally and theoretically to determine absolute enhancement factors. Thus, it continues to be an important goal both experimentally and theoretically to establish accurate determination of the enhancement magnitudes. However, we argue that it is equally important to move towards a better understanding of how the physical consequences of the enhancement mechanisms are reflected

in the SERS spectra. During the process of revealing the SERS enhancement mechanisms, computational modeling has been instrumental in advancing our understanding of SERS. To bridge computational modeling and experiments and exploit the full potential of SERS, more accurate description of the complex local environments needs to be addressed. This includes accounting for specific molecule-substrate interactions due to diffusion, orientation, field gradient effects and the presence of solvent/ligand as well as atomic details of the substrates. In addition, there is growing evidence that the EM and CM are strongly coupled and that it will be necessary to go beyond the traditional understanding of EM. The requirement for accurate description of the coupled mechanisms and the detailed local environments pose significant challenges to computational models. To overcome these challenges, the development of faster quantum mechanical methods,[295,296] quantum embedding methods[297–299] and machine learning models[300–302] are likely to be important future directions. We expect that the next generation computational toolbox will enable a more complete description of the enhancement mechanisms necessary to elucidate the full physical contents of SERS.

Acknowledgement

The authors gratefully acknowledge financial support from National Science Foundation Grant CHE-2106151 and CHE-2312222.

References

1. Moskovits, M. Surface-Enhanced Spectroscopy. *Rev. Mod. Phys.* **1985**, *57*, 783–826.

2. Campion, A.; Kambhampati, P. Surface-Enhanced Raman Scattering. *Chem. Soc. Rev.* **1998**, *27*, 241–250.

3. Kneipp, K.; Kneipp, H.; Itzkan, I.; Dasari, R. R.; Feld, M. S. Ultrasensitive Chemical Analysis by Raman Spectroscopy. *Chem. Rev.* **1999**, *99*, 2957–2976.

4. Link, S.; El-Sayed, M. A. Optical Properties and Ultrafast Dynamics of Metallic Nanocrystals. *Ann. Rev. Phys. Chem.* **2003**, *54*, 331–366.

5. Fleischmann, M.; Hendra, P.; McQuillan, A. Raman Spectra of Pyridine Adsorbed at a Silver Electrode. *Chem. Phys. Lett.* **1974**, *26*, 163–166.

6. Jeanmaire, D. L.; Van Duyne, R. P. Surface Raman Spectroelectrochemistry .1. Heterocyclic, Aromatic, and Aliphatic-Amines Adsorbed on Anodized Silver Electrode. *J. Electroanal. Chem.* **1977**, *84*, 1–20.

7. Albrecht, M. G.; Creighton, J. A. Anomalously Intense Raman Spectra of Pyridine at a Silver Electrode. *J. Am. Chem. Soc.* **1977**, *99*, 5215–5217.

8. Otto, A. Surface-Enhanced Raman Scattering of Adsorbates. *J. Raman Spectrosc.* **1991**, *22*, 743–752.

9. Kneipp, K.; Kneipp, H.; Itzkan, I.; Dasari, R. R.; Feld, M. S. Surface-Enhanced Raman Scattering and Biophysics. *J. Phys.: Condens. Matter* **2002**, *14*, R597.

10. Moskovits, M. Surface-Enhanced Raman Spectroscopy: A Brief Retrospective. *J. Raman Spectrosc.* **2005**, *36*, 485–496.

11. Stiles, P. L.; Dieringer, J. A.; Shah, N. C.; Van Duyne, R. P. Surface-Enhanced Raman Spectroscopy. *Annu. Rev. Anal. Chem.* **2008**, *1*, 601–626.

12. Michaels, A. M.; Nirmal, M.; Brus, L. E. Surface Enhanced Raman Spectroscopy of Individual Rhodamine 6G Molecules on Large Ag Nanocrystals. *J. Am. Chem. Soc.* **1999**, *121*, 9932–9939.

13. Xu, H.; Bjerneld, E. J.; Käll, M.; Börjesson, L. Spectroscopy of Single Hemoglobin Molecules by Surface Enhanced Raman Scattering. *Phys. Rev. Lett.* **1999**, *83*, 4357–4360.

14. Dieringer, J. A.; Lettan, R. B.; Scheidt, K. A.; Van Duyne, R. P. A Frequency Domain Existence Proof of Single-Molecule Surface-Enhanced Raman Spectroscopy. *J. Am. Chem. Soc.* **2007**, *129*, 16249–16256.

15. Kneipp, K.; Wang, Y.; Kneipp, H.; Perelman, L. T.; Itzkan, I.; Dasari, R. R.; Feld, M. S. Single Molecule Detection Using Surface-Enhanced Raman Scattering (SERS). *Phys. Rev. Lett.* **1997**, *78*, 1667–1670.

16. Nie, S. M.; Emory, S. R. Probing Single Molecules and Single Nanoparticles by Surface-Enhanced Raman Scattering. *Science* **1997**, *275*, 1102–1106.

17. Pettinger, B.; Ren, B.; Picardi, G.; Schuster, R.; Ertl, G. Nanoscale Probing of Adsorbed Species by Tip-Enhanced Raman Spectroscopy. *Phys. Rev. Lett.* **2004**, *92*, 096101.

18. Verma, P. Tip-Enhanced Raman Spectroscopy: Technique and Recent Advances. *Chem. Rev.* **2017**, *117*, 6447–6466.

19. Zhang, Z.; Sheng, S.; Wang, R.; Sun, M. Tip-Enhanced Raman Spectroscopy. *Anal. Chem.* **2016**, *88*, 9328–9346.

20. Wang, X.; Huang, S.-C.; Huang, T.-X.; Su, H.-S.; Zhong, J.-H.; Zeng, Z.-C.; Li, M.-H.; Ren, B. Tip-Enhanced Raman Spectroscopy for Surfaces and Interfaces. *Chem. Soc. Rev.* **2017**, *46*, 4020–4041.

21. Lee, J.; Crampton, K. T.; Tallarida, N.; Apkarian, V. A. Visualizing Vibrational Normal Modes of a Single Molecule with Atomically Confined Light. *Nature* **2019**, *568*, 78–82.

22. Zhang, R.; Zhang, Y.; Dong, Z. C.; Jiang, S.; Zhang, C.; Chen, L. G.; Zhang, L.; Liao, Y.; Aizpurua, J.; Luo, Y.; Yang, J. L.; Hou, J. G. Chemical Mapping of a Single Molecule by Plasmon-Enhanced Raman Scattering. *Nature* **2013**, *498*, 82–86.

23. Langer, J.; Jimenez de Aberasturi, D.; Aizpurua, J.; Alvarez-Puebla, R. A.; Auguié, B.; Baumberg, J. J.; Bazan, G. C.; Bell, S. E. J.; Boisen, A.; Brolo, A. G.; Choo, J.; Cialla-May, D.; Deckert, V.; Fabris, L.; Faulds, K.; García de Abajo, F. J.; Goodacre, R.; Graham, D.; Haes, A. J.; Haynes, C. L. *et al.* Present and Future of Surface–Enhanced Raman Scattering. *ACS Nano* **2020**, *14*, 28–117.

24. Zrimsek, A. B.; Chiang, N.; Mattei, M.; Zaleski, S.; McAnally, M. O.; Chapman, C. T.; Henry, A.-I.; Schatz, G. C.; Van Duyne, R. P. Single-Molecule Chemistry with Surface- and Tip-Enhanced Raman Spectroscopy. *Chem. Rev.* **2017**, *117*, 7583–7613.

25. Yang, S.; Dai, X.; Stogin, B. B.; Wong, T.-S. Ultrasensitive Surface-Enhanced Raman Scattering Detection in Common Fluids. *Proc. Natl. Acad. Sci. USA* **2016**, *113*, 268–273.

26. Benz, F.; Schmidt, M. K.; Dreismann, A.; Chikkaraddy, R.; Zhang, Y.; Demetriadou, A.; Carnegie, C.; Ohadi, H.; de Nijs, B.; Esteban, R.; Aizpurua, J.; Baumberg, J. J. Single-Molecule Optomechanics in "Picocavities". *Science* **2016**, *354*, 726–729.

27. Chen, J.; Ding, W.; Luo, Z.; Loo, B. H.; Yao, J. Probing Single Molecules and Molecular Aggregates: Raman Spectroscopic Advances. *J. Raman Spectrosc.* **2016**, *47*, 623–635.

28. Zrimsek, A. B.; Wong, N. L.; Van Duyne, R. P. Single Molecule Surface-Enhanced Raman Spectroscopy: A Critical Analysis of the Bianalyte versus Isotopologue Proof. *J. Phys. Chem. C* **2016**, *120*, 5133–5142.

29. Otto, A. In *Light Scattering in Solids IV: Electronics Scattering, Spin Effects, SERS, and Morphic Effects*; Cardona, M., Güntherodt, G., Eds.; Top. Appl. Phys.; Springer, Berlin/Heidelberg, 1984; Vol. 54; pp 289–418.

30. Schatz, G. C.; Van Duyne, R. P. In *Handbook of Vibrational Spectroscopy*;

Chalmers, J. M., Griffiths, P. R., Eds.; John Wiley and Sons, Ltd: New York, 2002; Vol. 1; pp 759–774.

31. Jensen, L.; Aikens, C. M.; Schatz, G. C. Electronic Structure Methods for Studying Surface–Enhanced Raman Scattering. *Chem. Soc. Rev.* **2008**, *37*, 1061–1073.

32. Morton, S. M.; Silverstein, D. W.; Jensen, L. Theoretical Studies of Plasmonics Using Electronic Structure Methods. *Chem. Rev.* **2011**, *111*, 3962–3994.

33. Chulhai, D. V.; Hu, Z.; Moore, J. E.; Chen, X.; Jensen, L. Theory of Linear and Nonlinear Surface-Enhanced Vibrational Spectroscopies. *Annu. Rev. Phys. Chem.* **2016**, *67*, 541–564.

34. Pérez-Jiménez, A. I.; Lyu, D.; Lu, Z.; Liu, G.; Ren, B. Surface-Enhanced Raman Spectroscopy: Benefits, Trade-Offs and Future Developments. *Chem. Sci.* **2020**, *11*, 4563–4577.

35. Jones, R. R.; Hooper, D. C.; Zhang, L.; Wolverson, D.; Valev, V. K. Raman Techniques: Fundamentals and Frontiers. *Nanoscale Res Lett* **2019**, *14*, 231.

36. Ding, S.-Y.; You, E.-M.; Tian, Z.-Q.; Moskovits, M. Electromagnetic Theories of Surface-Enhanced Raman Spectroscopy. *Chem. Soc. Rev.* **2017**, *46*, 4042–4076.

37. Camden, J. P.; Dieringer, J. A.; Wang, Y.; Masiello, D. J.; Marks, L. D.; Schatz, G. C.; Van Duyne, R. P. Probing the Structure of Single-Molecule Surface-Enhanced Raman Scattering Hot Spots. *J. Am. Chem. Soc.* **2008**, *130*, 12616–12617.

38. Le Ru, E. C.; Blackie, E.; Meyer, M.; Etchegoin, P. G. Surface Enhanced Raman Scattering Enhancement Factors: A Comprehensive Study. *J. Phys. Chem. C* **2007**, *111*, 13794–13803.

39. Cotton, T. M.; Schultz, S. G.; Van Duyne, R. P. Surface-Enhanced Resonance Raman

Scattering from Cytochrome c and Myoglobin Adsorbed on a Silver Electrode. *J. Am. Chem. Soc.* **1980**, *102*, 7960–7962.

40. Le Ru, E. C.; Auguié, B. Enhancement Factors: A Central Concept during 50 Years of Surface-Enhanced Raman Spectroscopy. *ACS Nano* **2024**, *18*, 9773–9783.

41. Gersten, J. I. The Effect of Surface Roughness on Surface Enhanced Raman Scattering. *J. Chem. Phys.* **1980**, *72*, 5779–5780.

42. Gersten, J. I. Rayleigh, Mie, and Raman Scattering by Molecules Adsorbed on Rough Surfaces. *J. Chem. Phys.* **1980**, *72*, 5780–5781.

43. Gersten, J.; Nitzan, A. Electromagnetic Theory of Enhanced Raman Scattering by Molecules Adsorbed on Rough Surfaces. *J. Chem. Phys.* **1980**, *73*, 3023–3037.

44. Schatz, G. C. Theoretical Studies of Surface–Enhanced Raman Scattering. *Acc. Chem. Res.* **1984**, *17*, 370–376.

45. Le Ru, E. C.; Etchegoin, P. G. Rigorous Justification of the $|E|4$ Enhancement Factor in Surface Enhanced Raman Spectroscopy. *Chem. Phys. Lett.* **2006**, *423*, 63–66.

46. Ausman, L. K.; Schatz, G. C. On the Importance of Incorporating Dipole Reradiation in the Modeling of Surface Enhanced Raman Scattering from Spheres. *J. Chem. Phys.* **2009**, *131*, 084708.

47. Efrima, S.; Metiu, H. Classical Theory of Light Scattering by an Adsorbed Molecule. I. Theory. *J. Chem. Phys.* **1979**, *70*, 1602–1613.

48. Le Ru, E. C.; Etchegoin, P. G. *Principles of Surface-Enhanced Raman Spectroscopy*; Elsevier, 2009.

49. Yamamoto, Y. S.; Ozaki, Y.; Itoh, T. Recent Progress and Frontiers in the Electromagnetic Mechanism of Surface-Enhanced Raman Scattering. *J. Photochem. Photobiol. C* **2014**, *21*, 81–104.

50. Zhang, Y.; Dong, Z.-C.; Aizpurua, J. Theoretical Treatment of Single-Molecule Scanning Raman Picoscopy in Strongly Inhomogeneous near Fields. *J. Raman Spectrosc.* **2021**, *52*, 296–309.

51. Moskovits, M.; DiLella, D. P.; Maynard, K. J. Surface Raman Spectroscopy of a Number of Cyclic Aromatic Molecules Adsorbed on Silver: Selection Rules and Molecular Reorientation. *Langmuir* **1988**, *4*, 67–76.

52. Sass, J. K.; Neff, H.; Moskovits, M.; Holloway, S. Electric Field Gradient Effects on the Spectroscopy of Adsorbed Molecules. *J. Phys. Chem.* **1981**, *85*, 621–623.

53. Moskovits, M.; DiLella, D. P. Surface-Enhanced Raman Spectroscopy of Benzene and Benzene-D6 Adsorbed on Silver. *J. Chem. Phys.* **1980**, *73*, 6068–6075.

54. Wolkow, R. A.; Moskovits, M. Benzene Adsorbed on Silver: An Electron Energy Loss and Surface-Enhanced Raman Study. *J. Chem. Phys.* **1986**, *84*, 5196–5199.

55. Le Ru, E. C.; Etchegoin, P. G.; Meyer, M. Enhancement Factor Distribution around a Single Surface–Enhanced Raman Scattering Hot Spot and Its Relation to Single Molecule Detection. *J. Chem. Phys.* **2006**, *125*, 204701.

56. McMahon, J. M.; Li, S.; Ausman, L. K.; Schatz, G. C. Modeling the Effect of Small Gaps in Surface-Enhanced Raman Spectroscopy. *J. Phys. Chem. C* **2012**, *116*, 1627–1637.

57. Ding, S.-Y.; Yi, J.; Li, J.-F.; Ren, B.; Wu, D.-Y.; Panneerselvam, R.; Tian, Z.-Q. Nanostructure-Based Plasmon-Enhanced Raman Spectroscopy for Surface Analysis of Materials. *Nat Rev Mater* **2016**, *1*, 1–16.

58. Hao, E.; Schatz, G. C. Electromagnetic Fields around Silver Nanoparticles and Dimers. *J. Chem. Phys.* **2004**, *120*, 357–366.

59. Chen, R.; Jensen, L. Interpreting Chemical Enhancements of Surface-Enhanced Raman Scattering. *Chem. Phys. Rev.* **2023**, *4*, 021305.

60. Pandey, P. K. K.; Schatz, G. C. A Detailed Analysis of the Raman Enhancement Mechanisms Associated with the Interaction of a Raman Scatterer with a Resonant Metal Cluster: Results for Lin–H2. *J. Chem. Phys.* **1984**, *80*, 2959–2972.

61. Moore, J. E.; Morton, S. M.; Jensen, L. Importance of Correctly Describing Charge-Transfer Excitations for Understanding the Chemical Effect in SERS. *J. Phys. Chem. Lett.* **2012**, *3*, 2470–2475.

62. Morton, S. M.; Jensen, L. Understanding the Molecule-Surface Chemical Coupling in SERS. *J. Am. Chem. Soc.* **2009**, *131*, 4090–4098.

63. Chen, R.; Jensen, L. Interpreting the Chemical Mechanism in SERS Using a Raman Bond Model. *J. Chem. Phys.* **2020**, *152*, 024126.

64. Jensen, L.; Zhao, L. L.; Schatz, G. C. Size-Dependence of the Enhanced Raman Scattering of Pyridine Adsorbed on Agn (n = 2-8, 20) Clusters. *J. Phys. Chem. C* **2007**, *111*, 4756–4764.

65. Zhao, L.; Jensen, L.; Schatz, G. C. Pyridine-Ag20 Cluster: A Model System for Studying Surface-Enhanced Raman Scattering. *J. Am. Chem. Soc.* **2006**, *128*, 2911–2919.

66. Xia, L.; Chen, M.; Zhao, X.; Zhang, Z.; Xia, J.; Xu, H.; Sun, M. Visualized Method of Chemical Enhancement Mechanism on SERS and TERS. *J. Raman Spectrosc.* **2014**, *45*, 533–540.

67. Afroosheh, S.; Zayak, A. T. Two Damping Mechanisms in the Chemically Enhanced Raman Scattering on Graphene: DFT Study. *J. Phys. Chem. C* **2020**, *124*, 24723–24730.

68. Zayak, A. T.; Hu, Y. S.; Choo, H.; Bokor, J.; Cabrini, S.; Schuck, P. J.; Neaton, J. B. Chemical Raman Enhancement of Organic Adsorbates on Metal Surfaces. *Phys. Rev. Lett.* **2011**, *106*, 083003.

69. Saikin, S. K.; Chu, Y.; Rappoport, D.; Crozier, K. B.; Aspuru-Guzik, A. Separation of Electromagnetic and Chemical Contributions to Surface-Enhanced Raman Spectra on Nanoengineered Plasmonic Substrates. *J. Phys. Chem. Lett.* **2010**, *1*, 2740–2746.

70. Valley, N.; Greeneltch, N.; Van Duyne, R. P.; Schatz, G. C. A Look at the Origin and Magnitude of the Chemical Contribution to the Enhancement Mechanism of Surface-Enhanced Raman Spectroscopy (SERS): Theory and Experiment. *J. Phys. Chem. Lett.* **2013**, *4*, 2599–2604.

71. Lombardi, J. R.; Birke, R. L. A Unified View of Surface-Enhanced Raman Scattering. *Acc. Chem.Res.* **2009**, *42*, 734–742.

72. Lombardi, J. R.; Birke, R. L. A Unified Approach to Surface-Enhanced Raman Spectroscopy. *J. Phys. Chem. C* **2008**, *112*, 5605–5617.

73. Hildebrandt, P.; Stockburger, M. Surface-Enhanced Resonance Raman Spectroscopy of Rhodamine 6G Adsorbed on Colloidal Silver. *J. Phys. Chem.* **1984**, *88*, 5935–5944.

74. Jensen, L.; Schatz, G. C. Resonance Raman Scattering of Rhodamine 6G as Calculated Using Time-Dependant Density Functional Theory. *J. Phys. Chem. A* **2006**, *110*, 5973–5977.

75. Fort, E.; Grésillon, S. Surface Enhanced Fluorescence. *J. Phys. D: Appl. Phys.* **2008**, *41*, 013001.

76. Amsterdam, S. H.; Stanev, T. K.; Zhou, Q.; Lou, A. J.-T.; Bergeron, H.; Darancet, P.; Hersam, M. C.; Stern, N. P.; Marks, T. J. Electronic Coupling in

Metallophthalocyanine–Transition Metal Dichalcogenide Mixed-Dimensional Heterojunctions. *ACS Nano* **2019**, *13*, 4183–4190.

77. Kim, J.; Jang, Y.; Kim, N.-J.; Kim, H.; Yi, G.-C.; Shin, Y.; Kim, M. H.; Yoon, S. Study of Chemical Enhancement Mechanism in Non-plasmonic Surface Enhanced Raman Spectroscopy (SERS). *Front. Chem.* **2019**, *7*, 582.

78. Itoh, T.; Procházka, M.; Dong, Z.-C.; Ji, W.; Yamamoto, Y. S.; Zhang, Y.; Ozaki, Y. Toward a New Era of SERS and TERS at the Nanometer Scale: From Fundamentals to Innovative Applications. *Chem. Rev.* **2023**, *123*, 1552–1634.

79. Bell, S. E. J.; Charron, G.; Cortés, E.; Kneipp, J.; de la Chapelle, M. L.; Langer, J.; Procházka, M.; Tran, V.; Schlücker, S. Towards Reliable and Quantitative Surface-Enhanced Raman Scattering (SERS): From Key Parameters to Good Analytical Practice. *Angew. Chem., Int. Edit.* **2020**, *59*, 5454–5462.

80. Fan, M.; Andrade, G. F. S.; Brolo, A. G. A Review on Recent Advances in the Applications of Surface-Enhanced Raman Scattering in Analytical Chemistry. *Anal. Chim. Acta.* **2020**, *1097*, 1–29.

81. Gao, Xiaoping.; Davies, J. P.; Weaver, M. J. Test of Surface Selection Rules for Surface-Enhanced Raman Scattering: The Orientation of Adsorbed Benzene and Monosubstituted Benzenes on Gold. *J. Phys. Chem.* **1990**, *94*, 6858–6864.

82. Creighton, J. Surface Raman Electromagnetic Enhancement Factors for Molecules at the Surface of Small Isolated Metal Spheres: The Determination of Adsorbate Orientation from Sers Relative Intensities. *Surf. Sci.* **1983**, *124*, 209–219.

83. Chen, R.; Jensen, L. Understanding Chemical Enhancements of Surface-Enhanced Raman Scattering Using a Raman Bond Model for Extended Systems. *J. Chem. Phys.* **2022**, *157*, 184705.

84. Le Ru, E. C.; Meyer, S. A.; Artur, C.; Etchegoin, P. G.; Grand, J.; Lang, P.; Maurel, F. Experimental Demonstration of Surface Selection Rules for SERS on Flat Metallic Surfaces. *Chem. Commun.* **2011**, *47*, 3903–3905.

85. Moskovits, M.; Suh, J. S. Surface Selection Rules for Surface-Enhanced Raman Spectroscopy: Calculations and Application to the Surface-Enhanced Raman Spectrum of Phthalazine on Silver. *J. Phys. Chem.* **1984**, *88*, 5526–5530.

86. Moskovits, M. Surface Selection Rules. *J. Chem. Phys.* **1982**, *77*, 4408–4416.

87. Marshall, A. R. L.; Roberts, M.; Gierschner, J.; Bouillard, J.-S. G.; Adawi, A. M. Probing the Molecular Orientation of a Single Conjugated Polymer via Nanogap SERS. *ACS Appl. Polym. Mater.* **2019**, *1*, 1175–1180.

88. Banik, M.; El-Khoury, P. Z.; Nag, A.; Rodriguez-Perez, A.; Guarrottxena, N.; Bazan, G. C.; Apkarian, V. A. Surface-Enhanced Raman Trajectories on a Nano-Dumbbell: Transition from Field to Charge Transfer Plasmons as the Spheres Fuse. *ACS Nano* **2012**, *6*, 10343–10354.

89. Allen, C. S.; van Duyne, R. P. Orientational Specificity of Raman Scattering from Molecules Adsorbed on Silver Electrodes. *Chem. Phys. Lett.* **1979**, *63*, 455–459.

90. El-Khoury, P. Z.; Johnson, G. E.; Novikova, I. V.; Gong, Y.; Joly, A. G.; Evans, J. E.; Zamkov, M.; Laskin, J.; Hess, W. P. Enhanced Raman Scattering from Aromatic Dithiols Electrosprayed into Plasmonic Nanojunctions. *Faraday Discuss.* **2015**, *184*, 339–357.

91. Kwon, Y. J.; Son, D. H.; Ahn, S. J.; Kim, M. S.; Kim, K. Vibrational Spectroscopic Investigation of Benzoic Acid Adsorbed on Silver. *J. Phys. Chem.* **1994**, *98*, 8481–8487.

92. Akbali, B.; Yagmurcukardes, M.; Peeters, F. M.; Lin, H.-Y.; Lin, T.-Y.; Chen, W.-H.; Maher, S.; Chen, T.-Y.; Huang, C.-H. Determining the Molecular Orientation on

the Metal Nanoparticle Surface through Surface-Enhanced Raman Spectroscopy and Density Functional Theory Simulations. *J. Phys. Chem. C* **2021**, *125*, 16289–16295.

93. Thimes, R. L.; Santos, A. V. B.; Chen, R.; Kaur, G.; Jensen, L.; Jenkins, D. M.; Camden, J. P. Using Surface-Enhanced Raman Spectroscopy to Unravel the Wingtip-Dependent Orientation of N-Heterocyclic Carbenes on Gold Nanoparticles. *J. Phys. Chem. Lett.* **2023**, *14*, 4219–4224.

94. Li, R.; Chaudhry, I.; Tseng, C.; Weng, S.; Wang, Y.; Zhao, B.; Aravind, I.; Cai, Z.; Dawlaty, J.; Jensen, L.; Cronin, S. B. SERS Detection of Charge Transfer at Electrochemical Interfaces Using Surface-Bound Ferrocene. *J. Phys. Chem. C* **2023**, *127*, 14263–14269.

95. Matthews, J. R.; Shirazinejad, C. R.; Isakson, G. A.; Demers, S. M. E.; Hafner, J. H. Structural Analysis by Enhanced Raman Scattering. *Nano Lett.* **2017**, *17*, 2172–2177.

96. El-Khoury, P. Z.; Aprà, E. Spatially Resolved Mapping of Three-Dimensional Molecular Orientations with ∼2 nm Spatial Resolution through Tip-Enhanced Raman Scattering. *J. Phys. Chem. C* **2020**, *124*, 17211–17217.

97. Van Dyck, C.; Fu, B.; Van Duyne, R. P.; Schatz, G. C.; Ratner, M. A. Deducing the Adsorption Geometry of Rhodamine 6G from the Surface-Induced Mode Renormalization in Surface-Enhanced Raman Spectroscopy. *J. Phys. Chem. C* **2018**, *122*, 465–473.

98. Chulhai, D. V.; Chen, X.; Jensen, L. Simulating Ensemble-Averaged Surface-Enhanced Raman Scattering. *J. Phys. Chem. C* **2016**, *120*, 20833–20842.

99. Khlebtsov, N. G.; Le Ru, E. C. Analytical Solutions for the Surface- and Orientation-Averaged SERS Enhancement Factor of Small Plasmonic Particles. *J. Raman Spectrosc.* **2021**, *52*, 285–295.

100. Becca, J. C.; Chen, X.; Jensen, L. A Discrete Interaction Model/Quantum Mechanical Method for Simulating Surface-Enhanced Raman Spectroscopy in Solution. *J. Chem. Phys.* **2021**, *154*, 224705.

101. Feibelman, P. J. Microscopic Calculation of Electromagnetic Fields in Refraction at a Jellium-Vacuum Interface. *Phys. Rev. B* **1975**, *12*, 1319–1336.

102. Payton, J. L.; Morton, S. M.; Moore, J. E.; Jensen, L. A Discrete Interaction Model/Quantum Mechanical Method for Simulating Surface-Enhanced Raman Spectroscopy. *J. Chem. Phys.* **2012**, *136*, 214103.

103. Liu, P.; Chen, X.; Ye, H.; Jensen, L. Resolving Molecular Structures with High-Resolution Tip-Enhanced Raman Scattering Images. *ACS Nano* **2019**, *13*, 9342–9351.

104. Chen, X.; Liu, P.; Hu, Z.; Jensen, L. High-Resolution Tip-Enhanced Raman Scattering Probes Sub-Molecular Density Changes. *Nat. Commun.* **2019**, *10*, 2567.

105. Takase, M.; Ajiki, H.; Mizumoto, Y.; Komeda, K.; Nara, M.; Nabika, H.; Yasuda, S.; Ishihara, H.; Murakoshi, K. Selection–Rule Breakdown in Plasmon–Induced Electronic Excitation of an Isolated Single–Walled Carbon Nanotube. *Nat. Photonics* **2013**, *7*, 550–554.

106. Aikens, C. M.; Madison, L. R.; Schatz, G. C. Raman Spectroscopy: The Effect of Field Gradient on SERS. *Nat. Photonics* **2013**, *7*, 508–510.

107. Chulhai, D. V.; Jensen, L. Determining Molecular Orientation With Surface-Enhanced Raman Scattering Using Inhomogenous Electric Fields. *J. Phys. Chem. C* **2013**, *117*, 19622–19631.

108. Janesko, B. G.; Scuseria, G. E. Surface Enhanced Raman Optical Activity of Molecules on Orientationally Averaged Substrates: Theory of Electromagnetic Effects. *J. Chem. Phys.* **2006**, *125*, 124704.

109. Golab, J. T.; Sprague, J. R.; Carron, K. T.; Schatz, G. C.; Van Duyne, R. P. A Surface Enhanced Hyper-Raman Scattering Study of Pyridine Adsorbed onto Silver: Experiment and Theory. *J. Chem. Phys.* **1988**, *88*, 7942–7951.

110. Turley, H. K.; Hu, Z.; Jensen, L.; Camden, J. P. Surface-Enhanced Resonance Hyper-Raman Scattering Elucidates the Molecular Orientation of Rhodamine 6G on Silver Colloids. *J. Phys. Chem. Lett.* **2017**, *8*, 1819–1823.

111. Chenal, C.; Birke, R. L.; Lombardi, J. R. Determination of the Degree of Charge-Transfer Contributions to Surface-Enhanced Raman Spectroscopy. *ChemPhysChem* **2008**, *9*, 1617–1623.

112. Avila, F.; Fernandez, D. J.; Arenas, J. F.; Otero, J. C.; Soto, J. Modelling the Effect of the Electrode Potential on the Metal–Adsorbate Surface States: Relevant States in the Charge Transfer Mechanism of SERS. *Chem. Commun.* **2011**, *47*, 4210–4212.

113. Dendisová, M.; Němečková, Z.; Člupek, M.; Prokopec, V. EC-SERS Study of Phenolic Acids Sorption Behavior on Au, Ag and Cu Substrates – Effect of Applied Potential and Metal Used. *Appl. Surf. Sci.* **2019**, *470*, 716–723.

114. Aranda, D.; García-González, F.; Avila Ferrer, F. J.; López-Tocón, I.; Soto, J.; Otero, J. C. Computational Model for Electrochemical Surface-Enhanced Raman Scattering: Key Role of the Surface Charges and Synergy between Electromagnetic and Charge-Transfer Enhancement Mechanisms. *J. Chem. Theory Comput.* **2022**, *18*, 6802–6815.

115. Yang, W.-H.; Schatz, G. C.; Van Duyne, R. P. Discrete Dipole Approximation for Calculating Extinction and Raman Intensities for Small Particles with Arbitrary Shapes. *J. Chem. Phys.* **1995**, *103*, 869–875.

116. Draine, B. T.; Flatau, P. J. Discrete-Dipole Approximation For Scattering Calculations. *J. Opt. Soc. Am. A* **1994**, *11*, 1491–1499.

117. Bian, R. X.; Dunn, R. C.; Xie, X. S.; Leung, P. T. Single Molecule Emission Characteristics in Near-Field Microscopy. *Phys. Rev. Lett.* **1995**, *75*, 4772–4775.

118. Kelly, K. L.; Coronado, E.; Zhao, L. L.; Schatz, G. C. The Optical Properties of Metal Nanoparticles: The Influence of Size, Shape, and Dielectric Environment. *J. Phys. Chem. B* **2003**, *107*, 668–677.

119. Corni, S.; Tomasi, J. Enhanced Response Properties of a Chromophore Physisorbed on a Metal Particle. *J. Chem. Phys.* **2001**, *114*, 3739–3751.

120. Corni, S.; Tomasi, J. Excitation Energies of a Molecule Close to a Metal Surface. *J. Chem. Phys.* **2002**, *117*, 7266–7278.

121. Lopata, K.; Neuhauser, D. Multiscale Maxwell–Schrödinger Modeling: A Split Field Finite-Difference Time-Domain Approach to Molecular Nanopolaritonics. *J. Chem. Phys.* **2009**, *130*, 104707.

122. Corni, S.; Tomasi, J. Surface Enhanced Raman Scattering from a Single Molecule Adsorbed on a Metal Particle Aggregate: A Theoretical Study. *J. Chem. Phys.* **2002**, *116*, 1156–1164.

123. Morton, S. M.; Jensen, L. A Discrete Interaction Model/Quantum Mechanical Method to Describe the Interaction of Metal Nanoparticles and Molecular Absorption. *J. Chem. Phys.* **2011**, *135*, 134103.

124. Giovannini, T.; Rosa, M.; Corni, S.; Cappelli, C. A Classical Picture of Subnanometer Junctions: An Atomistic Drude Approach to Nanoplasmonics. *Nanoscale* **2019**, *11*, 6004–6015.

125. Giovannini, T.; Bonatti, L.; Lafiosca, P.; Nicoli, L.; Castagnola, M.; Illobre, P. G.; Corni, S.; Cappelli, C. Do We Really Need Quantum Mechanics to Describe Plasmonic Properties of Metal Nanostructures? *ACS Photonics* **2022**, *9*, 3025–3034.

126. Saikin, S. K.; Olivares-Amaya, R.; Rappoport, D.; Stopa, M.; Aspuru-Guzik, A. On the Chemical Bonding Effects in the Raman Response: Benzenethiol Adsorbed on Silver Clusters. *Phys. Chem. Chem. Phys.* **2009**, *11*, 9401–9411.

127. Hu, W.; Duan, S.; Luo, Y. Theoretical Modeling of Surface and Tip-Enhanced Raman Spectroscopies. *WIREs Comput. Mol. Sci.* **2017**, *7*, e1293.

128. Zhao, X.; Chen, M. DFT Study on the Influence of Electric Field on Surface-Enhanced Raman Scattering from Pyridine–Metal Complex. *J. Raman Spectrosc.* **2014**, *45*, 62–67.

129. Johansson, P. Illustrative Direct Ab Initio Calculations of Surface Raman Spectra. *Phys. Chem. Chem. Phys.* **2005**, *7*, 475–482.

130. Wu, D.-Y.; Duan, S.; Ren, B.; Tian, Z.-Q. Density Functional Theory Study of Surface-Enhanced Raman Scattering Spectra of Pyridine Adsorbed on Noble and Transition Metal Surfaces. *J. Raman Spectrosc.* **2005**, *36*, 533–540.

131. Hu, W.; Duan, S.; Zhang, G.; Ma, Y.; Tian, G.; Luo, Y. Quasi-Analytical Approach for Modeling of Surface-Enhanced Raman Scattering. *J. Phys. Chem. C* **2015**, *119*, 28992–28998.

132. Birke, R. L.; Lombardi, J. R. Relative Contributions of Franck-Condon to Herzberg-Teller Terms in Charge Transfer Surface-Enhanced Raman Scattering Spectroscopy. *J. Chem. Phys.* **2020**, *152*, 224107.

133. Lombardi, J. R.; Birke, R. L.; Lu, T.; Xu, J. Charge-Transfer Theory of Surface Enhanced Raman Spectroscopy: Herzberg–Teller Contributions. *J. Chem. Phys.* **1986**, *84*, 4174–4180.

134. Lombardi, J. R.; Birke, R. L. Time-Dependent Picture of the Charge-Transfer Contributions to Surface Enhanced Raman Spectroscopy. *J. Chem. Phys.* **2007**, *126*, 244709.

135. Chen, R.; Jensen, L. Quantifying the Enhancement Mechanisms of Surface–Enhanced Raman Scattering Using a Raman Bond Model. *J. Chem. Phys.* **2020**, *153*, 224704.

136. Osawa, M.; Matsuda, N.; Yoshii, K.; Uchida, I. Charge Transfer Resonance Raman Process in Surface-Enhanced Raman Scattering from p-Aminothiophenol Adsorbed on Silver: Herzberg-teller Contribution. *J. Phys. Chem.* **1994**, *98*, 12702–12707.

137. Krajczewski, J.; Ambroziak, R.; Kudelski, A. Substrates for Surface-Enhanced Raman Scattering Formed on Nanostructured Non-Metallic Materials: Preparation and Characterization. *Nanomaterials* **2021**, *11*, 75.

138. Jin, S.; Zhang, D.; Yang, B.; Guo, S.; Chen, L.; Jung, Y. M. Noble Metal-Free SERS: Mechanisms and Applications. *Analyst* **2023**, *149*, 11–28.

139. Demirel, G.; Gieseking, R. L. M.; Ozdemir, R.; Kahmann, S.; Loi, M. A.; Schatz, G. C.; Facchetti, A.; Usta, H. Molecular Engineering of Organic Semiconductors Enables Noble Metal-Comparable SERS Enhancement and Sensitivity. *Nat. Commun.* **2019**, *10*, 5502.

140. Yilmaz, M.; Babur, E.; Ozdemir, M.; Gieseking, R. L.; Dede, Y.; Tamer, U.; Schatz, G. C.; Facchetti, A.; Usta, H.; Demirel, G. Nanostructured Organic Semiconductor Films for Molecular Detection with Surface-Enhanced Raman Spectroscopy. *Nat. Mater.* **2017**, *16*, 918–924.

141. Sun, H.; Gong, W.; Cong, S.; Liu, C.; Song, G.; Lu, W.; Zhao, Z. Ultrathin Two-Dimensional Metal–Organic Framework Nanosheets with Activated Ligand-Cluster Units for Enhanced SERS. *ACS Appl. Mater. Interfaces* **2022**, *14*, 2326–2334.

142. Sun, H.; Cong, S.; Zheng, Z.; Wang, Z.; Chen, Z.; Zhao, Z. Metal–Organic Frameworks as Surface Enhanced Raman Scattering Substrates with High Tailorability. *J. Am. Chem. Soc.* **2019**, *141*, 870–878.

143. Yu, Z.; Yu, W.; Xing, J.; Ganeev, R. A.; Xin, W.; Cheng, J.; Guo, C. Charge Transfer Effects on Resonance-Enhanced Raman Scattering for Molecules Adsorbed on Single-Crystalline Perovskite. *ACS Photonics* **2018**, *5*, 1619–1627.

144. Wang, X.-D.; Huang, Y.-H.; Liao, J.-F.; Jiang, Y.; Zhou, L.; Zhang, X.-Y.; Chen, H.-Y.; Kuang, D.-B. In Situ Construction of a Cs2SnI6 Perovskite Nanocrystal/SnS2 Nanosheet Heterojunction with Boosted Interfacial Charge Transfer. *J. Am. Chem. Soc.* **2019**, *141*, 13434–13441.

145. Zheng, J.; Dai, B.; Liu, J.; Liu, J.; Ji, m.; Liu, J.; Zhou, Y.; Xu, M.; Zhang, J. Hierarchical Self-Assembly of Cu7Te5 Nanorods into Superstructures with Enhanced SERS Performance. *ACS Appl. Mater. Interfaces* **2016**, *8*, 35426–35434.

146. Ling, X.; Fang, W.; Lee, Y.-H.; Araujo, P. T.; Zhang, X.; Rodriguez-Nieva, J. F.; Lin, Y.; Zhang, J.; Kong, J.; Dresselhaus, M. S. Raman Enhancement Effect on Two-Dimensional Layered Materials: Graphene, h-BN and MoS2. *Nano Lett.* **2014**, *14*, 3033–3040.

147. Muehlethaler, C.; Considine, C. R.; Menon, V.; Lin, W.-C.; Lee, Y.-H.; Lombardi, J. R. Ultrahigh Raman Enhancement on Monolayer MoS2. *ACS Photonics* **2016**, *3*, 1164–1169.

148. Yin, Y.; Miao, P.; Zhang, Y.; Han, J.; Zhang, X.; Gong, Y.; Gu, L.; Xu, C.; Yao, T.; Xu, P.; Wang, Y.; Song, B.; Jin, S. Significantly Increased Raman Enhancement on MoX2 (X = S, Se) Monolayers upon Phase Transition. *Adv. Funct. Mater.* **2017**, *27*, 1606694.

149. Song, X.; Wang, Y.; Zhao, F.; Li, Q.; Ta, H. Q.; Rümmeli, M. H.; Tully, C. G.; Li, Z.; Yin, W.-J.; Yang, L.; Lee, K.-B.; Yang, J.; Bozkurt, I.; Liu, S.; Zhang, W.; Chhowalla, M. Plasmon-Free Surface-Enhanced Raman Spectroscopy Using Metallic 2D Materials. *ACS Nano* **2019**, *13*, 8312–8319.

150. Xu, H.; Chen, Y.; Xu, W.; Zhang, H.; Kong, J.; Dresselhaus, M. S.; Zhang, J. Modulating the Charge-Transfer Enhancement in GERS Using an Electrical Field under Vacuum and an n/p-Doping Atmosphere. *Small* **2011**, *7*, 2945–2952.

151. Hao, Q.; Morton, S. M.; Wang, B.; Zhao, Y.; Jensen, L.; Jun Huang, T. Tuning Surface-Enhanced Raman Scattering from Graphene Substrates Using the Electric Field Effect and Chemical Doping. *Appl. Phys. Lett.* **2013**, *102*, 011102.

152. Jung, N.; Crowther, A. C.; Kim, N.; Kim, P.; Brus, L. Raman Enhancement on Graphene: Adsorbed and Intercalated Molecular Species. *ACS Nano* **2010**, *4*, 7005–7013.

153. Yu, X.; Cai, H.; Zhang, W.; Li, X.; Pan, N.; Luo, Y.; Wang, X.; Hou, J. G. Tuning Chemical Enhancement of SERS by Controlling the Chemical Reduction of Graphene Oxide Nanosheets. *ACS Nano* **2011**, *5*, 952–958.

154. Bontempi, N.; Carletti, L.; De Angelis, C.; Alessandri, I. Plasmon-Free SERS Detection of Environmental CO $_2$ on TiO $_2$ Surfaces. *Nanoscale* **2016**, *8*, 3226–3231.

155. Hayashi, S.; Koh, R.; Ichiyama, Y.; Yamamoto, K. Evidence for Surface-Enhanced Raman Scattering on Nonmetallic Surfaces: Copper Phthalocyanine Molecules on GaP Small Particles. *Phys. Rev. Lett.* **1988**, *60*, 1085–1088.

156. Wang, Y.; Liu, J.; Ozaki, Y.; Xu, Z.; Zhao, B. Effect of TiO2 on Altering Direction of Interfacial Charge Transfer in a TiO2-Ag-MPY-FePc System by SERS. *Angew. Chem. Int. Ed.* **2019**, *58*, 8172–8176.

157. Lombardi, J. R.; Birke, R. L. Theory of Surface-Enhanced Raman Scattering in Semiconductors. *J. Phys. Chem. C* **2014**, *118*, 11120–11130.

158. Sun, H.; Yao, M.; Song, Y.; Zhu, L.; Dong, J.; Liu, R.; Li, P.; Zhao, B.; Liu, B.

Pressure-Induced SERS Enhancement in a MoS $_2$ /Au/R6G System by a Two-Step Charge Transfer Process. *Nanoscale* **2019**, *11*, 21493–21501.

159. Sun, H.; Yu, H.; Han, B.; Ma, J.; Wang, R.; Song, Y. Pressure-Induced SERS-Enhanced Sensing of 4-Mercaptobenzoic Acid Using Few-Layer WS2 Nanosheets. *ACS Appl. Nano Mater.* **2023**, *6*, 7553–7561.

160. Wang, Y.; Ruan, W.; Zhang, J.; Yang, B.; Xu, W.; Zhao, B.; Lombardi, J. R. Direct Observation of Surface-Enhanced Raman Scattering in ZnO Nanocrystals. *J. Raman Spectrosc.* **2009**, *40*, 1072–1077.

161. Qi, D.; Lu, L.; Wang, L.; Zhang, J. Improved SERS Sensitivity on Plasmon-Free TiO2 Photonic Microarray by Enhancing Light-Matter Coupling. *J. Am. Chem. Soc.* **2014**, *136*, 9886–9889.

162. Tao, L.; Chen, K.; Chen, Z.; Cong, C.; Qiu, C.; Chen, J.; Wang, X.; Chen, H.; Yu, T.; Xie, W.; Deng, S.; Xu, J.-B. 1T′ Transition Metal Telluride Atomic Layers for Plasmon-Free SERS at Femtomolar Levels. *J. Am. Chem. Soc.* **2018**, *140*, 8696–8704.

163. Wang, X.; She, G.; Xu, H.; Mu, L.; Shi, W. The Surface-Enhanced Raman Scattering from ZnO Nanorod Arrays and Its Application for Chemosensors. *Sensors and Actuators B: Chemical* **2014**, *193*, 745–751.

164. Musumeci, A.; Gosztola, D.; Schiller, T.; Dimitrijevic, N. M.; Mujica, V.; Martin, D.; Rajh, T. SERS of Semiconducting Nanoparticles (TiO2 Hybrid Composites). *J. Am. Chem. Soc.* **2009**, *131*, 6040–6041.

165. Yang, Y.; O'Riordan, A.; Lovera, P. Highly Sensitive Pesticide Detection Using Electrochemically Prepared Silver-Gum Arabic Nanocluster SERS Substrates. *Sensors and Actuators B: Chemical* **2022**, *364*, 131851.

166. Huh, S.; Park, J.; Kim, Y. S.; Kim, K. S.; Hong, B. H.; Nam, J.-M. UV/Ozone-Oxidized Large-Scale Graphene Platform with Large Chemical Enhancement in Surface-Enhanced Raman Scattering. *ACS Nano* **2011**, *5*, 9799–9806.

167. Xu, H.; Xie, L.; Zhang, H.; Zhang, J. Effect of Graphene Fermi Level on the Raman Scattering Intensity of Molecules on Graphene. *ACS Nano* **2011**, *5*, 5338–5344.

168. Wang, X.; Shi, W.; She, G.; Mu, L. Using Si and Ge Nanostructures as Substrates for Surface-Enhanced Raman Scattering Based on Photoinduced Charge Transfer Mechanism. *J. Am. Chem. Soc.* **2011**, *133*, 16518–16523.

169. Ling, X.; Xie, L.; Fang, Y.; Xu, H.; Zhang, H.; Kong, J.; Dresselhaus, M. S.; Zhang, J.; Liu, Z. Can Graphene Be Used as a Substrate for Raman Enhancement? *Nano Lett.* **2010**, *10*, 553–561.

170. Kitadai, H.; Tan, Q.; Ping, L.; Ling, X. Raman Enhancement Induced by Exciton Hybridization in Molecules and 2D Materials. *npj 2D Mater Appl* **2024**, *8*, 1–8.

171. Lombardi, J. R. The Theory of Surface-Enhanced Raman Scattering on Semiconductor Nanoparticles; toward the Optimization of SERS Sensors. *Faraday Discuss.* **2017**, *205*, 105–120.

172. Islam, S. K.; Tamargo, M.; Moug, R.; Lombardi, J. R. Surface-Enhanced Raman Scattering on a Chemically Etched ZnSe Surface. *J. Phys. Chem. C* **2013**, *117*, 23372–23377.

173. Jiang, L.; You, T.; Yin, P.; Shang, Y.; Zhang, D.; Guo, L.; Yang, S. Surface-Enhanced Raman Scattering Spectra of Adsorbates on Cu2O Nanospheres: Charge-Transfer and Electromagnetic Enhancement. *Nanoscale* **2013**, *5*, 2784–2789.

174. Fu, X.; Jiang, T.; Zhao, Q.; Yin, H. Charge-Transfer Contributions in Surface-Enhanced

Raman Scattering from Ag, Ag2S and Ag2Se Substrates. *J. Raman Spectrosc.* **2012**, *43*, 1191–1195.

175. Wang, X.; Shi, W.; Jin, Z.; Huang, W.; Lin, J.; Ma, G.; Li, S.; Guo, L. Remarkable SERS Activity Observed from Amorphous ZnO Nanocages. *Angew. Chem. Int. Ed.* **2017**, *56*, 9851–9855.

176. Yang, L.; Peng, Y.; Yang, Y.; Liu, J.; Huang, H.; Yu, B.; Zhao, J.; Lu, Y.; Huang, Z.; Li, Z.; Lombardi, J. R. A Novel Ultra-Sensitive Semiconductor SERS Substrate Boosted by the Coupled Resonance Effect. *Adv. Sci.* **2019**, *6*, 1900310.

177. Ji, W.; Li, L.; Song, W.; Wang, X.; Zhao, B.; Ozaki, Y. Enhanced Raman Scattering by ZnO Superstructures: Synergistic Effect of Charge Transfer and Mie Resonances. *Angew. Chem. Int. Ed.* **2019**, *58*, 14452–14456.

178. Zheng, Z.; Cong, S.; Gong, W.; Xuan, J.; Li, G.; Lu, W.; Geng, F.; Zhao, Z. Semiconductor SERS Enhancement Enabled by Oxygen Incorporation. *Nat Commun* **2017**, *8*, 1993.

179. Ling, X.; Huang, S.; Deng, S.; Mao, N.; Kong, J.; Dresselhaus, M. S.; Zhang, J. Lighting Up the Raman Signal of Molecules in the Vicinity of Graphene Related Materials. *Acc. Chem. Res.* **2015**, *48*, 1862–1870.

180. Ling, X.; Wu, J.; Xu, W.; Zhang, J. Probing the Effect of Molecular Orientation on the Intensity of Chemical Enhancement Using Graphene-Enhanced Raman Spectroscopy. *Small* **2012**, *8*, 1365–1372.

181. Birke, R. L.; Lombardi, J. R. TDDFT Study of Charge-Transfer Raman Spectra of 4-Mercaptopyridine on Various ZnSe Nanoclusters as a Model for the SERS of 4-Mpy on Semiconductors. *J. Phys. Chem. C* **2018**, *122*, 4908–4927.

182. Hilty, F. W.; Kuhlman, A. K.; Pauly, F.; Zayak, A. T. Raman Scattering from a Molecule–Semiconductor Interface Tuned by an Electric Field: Density Functional Theory Approach. *J. Phys. Chem. C* **2015**, *119*, 23113–23118.

183. Dreuw, A.; Head-Gordon, M. Failure of Time-Dependent Density Functional Theory for Long-Range Charge-Transfer Excited States: The Zincbacteriochlorin-Bacteriochlorin and Bacteriochlorophyll-Spheroidene Complexes. *J. Am. Chem. Soc.* **2003**, *126*, 4007–4016.

184. Maitra, N. T. Charge Transfer in Time-Dependent Density Functional Theory. *J. Phys.: Condens. Matter* **2017**, *29*, 423001.

185. Casida, M.; Huix-Rotllant, M. Progress in Time-Dependent Density-Functional Theory. *Annu. Rev. Phys. Chem.* **2012**, *63*, 287–323.

186. Etchegoin, P. G.; Le Ru, E. C. Resolving Single Molecules in Surface–Enhanced Raman Scattering within the Inhomogeneous Broadening of Raman Peaks. *Anal. Chem.* **2010**, *82*, 2888–2892.

187. Griffiths, J.; Földes, T.; de Nijs, B.; Chikkaraddy, R.; Wright, D.; Deacon, W. M.; Berta, D.; Readman, C.; Grys, D.-B.; Rosta, E.; Baumberg, J. J. Resolving Sub–Angstrom Ambient Motion through Reconstruction from Vibrational Spectra. *Nat. Commun.* **2021/11/19, 2021**, *12*, 6759.

188. Sonntag, Matthew. D.; Chulhai, D.; Seideman, T.; Jensen, L.; Van Duyne, R. P. The Origin of Relative Intensity Fluctuations in Single–Molecule Tip–Enhanced Raman Spectroscopy. *J. Am. Chem. Soc.* **2013**, *135*, 17187–17192.

189. Baumberg, J. J.; Aizpurua, J.; Mikkelsen, M. H.; Smith, D. R. Extreme Nanophotonics from Ultrathin Metallic Gaps. *Nat. Mater.* **2019**, *18*, 668–678.

190. Sawai, Y.; Takimoto, B.; Nabika, H.; Ajito, K.; Murakoshi, K. Observation of a Small Number of Molecules at a Metal Nanogap Arrayed on a Solid Surface Using Surface-Enhanced Raman Scattering. *J. Am. Chem. Soc.* **2007**, *129*, 1658–1662.

191. Etchegoin, P. G.; Le Ru, E. C. A Perspective on Single Molecule SERS: Current Status and Future Challenges. *Phys. Chem. Chem. Phys.* **2008**, *10*, 6079–6089.

192. Blackie, E. J.; Le Ru, E. C.; Etchegoin, P. G. Single-Molecule Surface-Enhanced Raman Spectroscopy of Nonresonant Molecules. *J. Am. Chem. Soc.* **2009**, *131*, 14466–14472.

193. Goulet, P. J. G.; Aroca, R. F. Distinguishing Individual Vibrational Fingerprints: Single-molecule Surface-Enhanced Resonance Raman Scattering from One-to-One Binary Mixtures in Langmuir-Blodgett Monolayers. *Anal. Chem.* **2007**, *79*, 2728–2734.

194. Jaculbia, R. B.; Imada, H.; Miwa, K.; Iwasa, T.; Takenaka, M.; Yang, B.; Kazuma, E.; Hayazawa, N.; Taketsugu, T.; Kim, Y. Single-Molecule Resonance Raman Effect in a Plasmonic Nanocavity. *Nat. Nanotechnol.* **2020**, *15*, 105–110.

195. Al-Shammari, R. M.; Al-attar, N.; Manzo, M.; Gallo, K.; Rodriguez, B. J.; Rice, J. H. Single-Molecule Nonresonant Wide-Field Surface-Enhanced Raman Scattering from Ferroelectrically Defined Au Nanoparticle Microarrays. *ACS Omega* **2018**, *3*, 3165–3172.

196. Sonntag, M. D.; Klingsporn, J. M.; Garibay, L. K.; Roberts, J. M.; Dieringer, J. A.; Seideman, T.; Scheidt, K. A.; Jensen, L.; Schatz, G. C.; Van Duyne, R. P. Single-Molecule Tip-Enhanced Raman Spectroscopy. *J. Phys. Chem. C* **2012**, *116*, 478–483.

197. Stadler, J.; Schmid, T.; Zenobi, R. Nanoscale Chemical Imaging Using Top-Illumination Tip-Enhanced Raman Spectroscopy. *Nano Lett.* **2010**, *10*, 4514–4520.

198. Weiss, A.; Haran, G. Time-Dependent Single-Molecule Raman Scattering as a Probe of Surface Dynamics. *J. Phys. Chem. B* **2001**, *105*, 12348–12354.

199. Jiang, N.; Chiang, N.; Madison, L. R.; Pozzi, E. A.; Wasielewski, M. R.; Seideman, T.; Ratner, M. A.; Hersam, M. C.; Schatz, G. C.; Van Duyne, R. P. Nanoscale Chemical Imaging of a Dynamic Molecular Phase Boundary with Ultrahigh Vacuum Tip-Enhanced Raman Spectroscopy. *Nano Lett.* **2016**, *16*, 3898–3904.

200. Chen, H.-Y.; Lin, M.-H.; Wang, C.-Y.; Chang, Y.-M.; Gwo, S. Large-Scale Hot Spot Engineering for Quantitative SERS at the Single-Molecule Scale. *J. Am. Chem. Soc.* **2015**, *137*, 13698–13705.

201. Kang, M.; Kim, H.; Oleiki, E.; Koo, Y.; Lee, H.; Joo, H.; Choi, J.; Eom, T.; Lee, G.; Suh, Y. D.; Park, K.-D. Conformational Heterogeneity of Molecules Physisorbed on a Gold Surface at Room Temperature. *Nat Commun* **2022**, *13*, 4133.

202. Aprà, E.; Bhattarai, A.; El-Khoury, P. Z. Gauging Molecular Orientation through Time Domain Simulations of Surface-Enhanced Raman Scattering. *J. Phys. Chem. A* **2019**, *123*, 7142–7147.

203. Fischer, S. A.; Aprà, E.; Govind, N.; Hess, W. P.; El-Khoury, P. Z. Nonequilibrium Chemical Effects in Single-Molecule SERS Revealed by Ab Initio Molecular Dynamics Simulations. *J. Phys. Chem. A* **2017**, *121*, 1344–1350.

204. Fang, Y.; Seong, N.-H.; Dlott, D. D. Measurement of the Distribution of Site Enhancements in Surface-Enhanced Raman Scattering. *Science* **2008**, *321*, 388–392.

205. Mary, Y. S.; Mary, Y. S.; Armaković, S.; Armaković, S. J.; Krátký, M.; Vinsova, J.; Baraldi, C.; Gamberini, M. C. Concentration and Solvent Dependent SERS, DFT, MD Simulations and Molecular Docking Studies of a Thioxothiazolidine Derivative with Antimicrobial Properties. *J. Mol. Liq.* **2021**, *329*, 115582.

206. Tarakeshwar, P.; Finkelstein-Shapiro, D.; Hurst, S. J.; Rajh, T.; Mujica, V. Surface-Enhanced Raman Scattering on Semiconducting Oxide Nanoparticles: Oxide Nature, Size, Solvent, and pH Effects. *J. Phys. Chem. C* **2011**, *115*, 8994–9004.

207. Tarakeshwar, P.; Finkelstein-Shapiro, D.; Rajh, T.; Mujica, V. Quantum Confinement Effects on the Surface Enhanced Raman Spectra of Hybrid Systems Molecule-TiO2 Nanoparticles. *Int. J. Quantum Chem.* **2011**, *111*, 1659–1670.

208. Orozco-Gonzalez, Y.; Tarakeshwar, P.; Canuto, S.; Mujica, V. Solvent Effects on the Dynamic Polarizability and Raman Response of Molecule–Metal Oxide Hybrid Clusters. *ChemPhysChem* **2016**, *17*, 2590–2595.

209. Yamada, A. Molecular Simulation Study of Surface-Enhanced Raman Scattering of Liquid Water. *J. Phys. Chem. A* **2024**, *128*, 51–61.

210. Chen, X.; Moore, J. E.; Zekarias, M.; Jensen, L. Atomistic Electrodynamics Simulations of Bare and Ligand-Coated Nanoparticles in the Quantum Size Regime. *Nat. Commun.* **2015**, *6*, 8921.

211. Malola, S.; Lehtovaara, L.; Enkovaara, J.; Häkkinen, H. Birth of the Localized Surface Plasmon Resonance in Monolayer-Protected Gold Nanoclusters. *ACS Nano* **2013**, *7*, 10263–10270.

212. Chakraborty, I.; Govindarajan, A.; Erusappan, J.; Ghosh, A.; Pradeep, T.; Yoon, B.; Whetten, R. L.; Landman, U. The Superstable 25 kDa Monolayer Protected Silver Nanoparticle: Measurements and Interpretation as an Icosahedral Ag152(SCH2CH2Ph)60 Cluster. *Nano Lett.* **2012**, *12*, 5861–5866.

213. Cheng, W.; Dong, S.; Wang, E. Iodine-Induced Gold-Nanoparticle Fusion/Fragmentation/Aggregation and Iodine-Linked Nanostructured Assemblies on a Glass Substrate. *Angew. Chem., Int. Ed.* **2003**, *42*, 449–452.

214. Zhang, Z.; Li, H.; Zhang, F.; Wu, Y.; Guo, Z.; Zhou, L.; Li, J. Investigation of Halide-Induced Aggregation of Au Nanoparticles into Spongelike Gold. *Langmuir* **2014**, *30*, 2648–2659.

215. Stefancu, A.; Iancu, S. D.; Leopold, N. Selective Single Molecule SERRS of Cationic and Anionic Dyes by Cl– and Mg2+ Adions: An Old New Idea. *J. Phys. Chem. C* **2021**, *125*, 12802.

216. Xie, L.; Lu, J.; Liu, T.; Chen, G.; Liu, G.; Ren, B.; Tian, Z. Key Role of Direct Adsorption on SERS Sensitivity: Synergistic Effect among Target, Aggregating Agent, and Surface with Au or Ag Colloid as Surface-Enhanced Raman Spectroscopy Substrate. *J. Phys. Chem. Lett.* **2020**, *11*, 1022.

217. Liu, Y.; Liu, L.; Guo, R. Br–Induced Facile Fabrication of Spongelike Gold/Amino Acid Nanocomposites and Their Applications in Surface-Enhanced Raman Scattering. *Langmuir* **2010**, *26*, 13479–13485.

218. Zhang, Y.; Prabakar, S.; Le Ru, E. C. Coadsorbed Species with Halide Ligands on Silver Nanoparticles with Different Binding Affinities. *J. Phys. Chem. C* **2022**, *126*, 8692–8702.

219. Doering, W. E.; Nie, S. Single-Molecule and Single-Nanoparticle SERS: Examining the Roles of Surface Active Sites and Chemical Enhancement. *J. Phys. Chem. B* **2002**, *106*, 311–317.

220. Muniz-Miranda, M.; Sbrana, G. Evidence for Surface Ag+ Complex Formation by an Anion-Induced Effect in the SER Spectra of Phthalazine Adsorbed on Silver Sols. *J. Raman Spectrosc.* **1996**, *27*, 105.

221. Perera, G. S.; LaCour, A.; Zhou, Y.; Henderson, K. L.; Zou, S.; Perez, F.; Emerson, J. P.; Zhang, D. Iodide-Induced Organothiol Desorption and Photochemical Reaction, Gold Nanoparticle (AuNP) Fusion, and SERS Signal Reduction in Organothiol-Containing AuNP Aggregates. *J. Phys. Chem. C* **2015**, *119*, 4261.

222. Ansar, S. M.; Ameer, F. S.; Hu, W.; Zou, S.; Pittman, C. U.; Zhang, D. Removal

of Molecular Adsorbates on Gold Nanoparticles Using Sodium Borohydride in Water. *Nano Lett.* **2013**, *13*, 1226.

223. Stefancu, A.; Lee, S.; Zhu, L.; Liu, M.; Lucacel, R. C.; Cortés, E.; Leopold, N. Fermi Level Equilibration at the Metal–Molecule Interface in Plasmonic Systems. *Nano Lett.* **2021**, *21*, 6592.

224. Stefancu, A.; Biro, O. M.; Todor-Boer, O.; Botiz, I.; Cortés, E.; Leopold, N. Halide–Metal Complexes at Plasmonic Interfaces Create New Decay Pathways for Plasmons and Excited Molecules. *ACS Photonics* **2022**, *9*, 895–904.

225. Pang, R.; Zhang, X.-G.; Zhou, J.-Z.; Wu, D.-Y.; Tian, Z.-Q. SERS Chemical Enhancement of Water Molecules from Halide Ion Coadsorption and Photoinduced Charge Transfer on Silver Electrodes. *J. Phys. Chem. C* **2017**, *121*, 10445.

226. Tian, Z.-Q.; Ren, B. Adsorption and Reaction at Electrochemical Interfaces as Probed by Surface-Enhanced Raman Spectroscopy. *Annu. Rev. Phys. Chem.* **2004**, *55*, 197–229.

227. Karaballi, R. A.; Nel, A.; Krishnan, S.; Blackburn, J.; Brosseau, C. L. Development of an Electrochemical Surface-Enhanced Raman Spectroscopy (EC-SERS) Aptasensor for Direct Detection of DNA Hybridization. *Phys. Chem. Chem. Phys.* **2015**, *17*, 21356–21363.

228. Wu, D.-Y.; Li, J.-F.; Ren, B.; Tian, Z.-Q. Electrochemical Surface–Enhanced Raman Spectroscopy of Nanostructures. *Chem. Soc. Rev.* **2008**, *37*, 1025–1041.

229. Aranda, D.; Valdivia, S.; Soto, J.; López-Tocón, I.; Avila, F. J.; Otero, J. C. Theoretical Approaches for Modeling the Effect of the Electrode Potential in the SERS Vibrational Wavenumbers of Pyridine Adsorbed on a Charged Silver Surface. *Front. Chem.* **2019**, *7*.

230. Fiocco, A.; Pavlic, A. A.; Kanoufi, F.; Maisonhaute, E.; Noël, J.-M.; Lucas, I. T. Electrochemical Tip-Enhanced Raman Spectroscopy for the Elucidation of Complex Electrochemical Reactions. *Anal. Chem.* **2024**, *96*, 2791–2798.

231. Cortés, E.; Etchegoin, P. G.; Le Ru, E. C.; Fainstein, A.; Vela, M. E.; Salvarezza, R. C. Monitoring the Electrochemistry of Single Molecules by Surface-Enhanced Raman Spectroscopy. *J. Am. Chem. Soc.* **2010**, *132*, 18034–18037.

232. Mohammadpour, M.; Khodabandeh, M. H.; Visscher, L.; Jamshidi, Z. Elucidation of Charge-Transfer SERS Selection Rules by Considering the Excited State Properties and the Role of Electrode Potential. *Phys. Chem. Chem. Phys.* **2017**, *19*, 7833–7843.

233. Marr, J. M.; Schultz, Z. D. Imaging Electric Fields in SERS and TERS Using the Vibrational Stark Effect. *J. Phys. Chem. Lett.* **2013**, *4*, 3268–3272.

234. Oklejas, V.; Sjostrom, C.; Harris, J. M. SERS Detection of the Vibrational Stark Effect from Nitrile-Terminated SAMs to Probe Electric Fields in the Diffuse Double-Layer. *J. Am. Chem. Soc.* **2002**, *124*, 2408–2409.

235. Oklejas, V.; Sjostrom, C.; Harris, J. M. Surface-Enhanced Raman Scattering Based Vibrational Stark Effect as a Spatial Probe of Interfacial Electric Fields in the Diffuse Double Layer. *J. Phys. Chem. B* **2003**, *107*, 7788–7794.

236. Kurouski, D.; Mattei, M.; Duyne, R. P. V. Probing Redox Reactions at the Nanoscale with Electrochemical Tip-Enhanced Raman Spectroscopy. *Nano Lett.* **2015**, *15*, 7956–7962.

237. Sanchez, L. A.; Birke, R. L.; Lombardi, J. R. Surface-Enhanced Raman Scattering of Piperidine. The Effect of Electrode Potential on Intensity. *J. Phys. Chem.* **1984**, *88*, 1762–1766.

238. Brolo, A. G.; Jiang, Z.; Irish, D. E. The Orientation of 2,2*ı*-Bipyridine Adsorbed at a SERS-active Au(1 1 1) Electrode Surface. *J. Electroanal. Chem.* **2003**, *547*, 163–172.

239. Li, X.; Gewirth, A. A. Potential-Dependent Reorientation of Thiocyanate on Au Electrodes. *J. Am. Chem. Soc.* **2003**, *125*, 11674–11683.

240. Poonia, M.; Küster, T.; Bothun, G. D. Organic Anion Detection with Functionalized SERS Substrates via Coupled Electrokinetic Preconcentration, Analyte Capture, and Charge Transfer. *ACS Appl. Mater. Interfaces* **2022**, *14*, 23964–23972.

241. Chase, B.; Parkinson, B. A Study of the Wavelength and Potential Dependence of Surface Enhanced Raman Scattering on Copper, Silver, and Gold Electrodes. *J. Phys. Chem.* **1991**, *95*, 7810–7813.

242. Román-Pérez, J.; López-Tocón, I.; Castro, J. L.; Arenas, J. F.; Soto, J.; Otero, J. C. The Electronic Structure of Metal–Molecule Hybrids in Charged Interfaces: Surface-Enhanced Raman Selection Rules Derived from Plasmon-like Resonances. *Phys. Chem. Chem. Phys.* **2014**, *17*, 2326–2329.

243. Arenas, J. F.; Fernández, D. J.; Soto, J.; López-Tocón, I.; Otero, J. C. Role of the Electrode Potential in the Charge-Transfer Mechanism of Surface-Enhanced Raman Scattering. *J. Phys. Chem. B* **2003**, *107*, 13143–13149.

244. Roman-Perez, J.; Ruano, C.; Centeno, S. P.; López-Tocón, I.; Arenas, J. F.; Soto, J.; Otero, J. C. Huge Energy Gain in Metal-to-Molecule Charge Transfer Processes: A Combined Effect of an Electrical Capacitive Enhancement in Nanometer-Size Hot Spots and the Electronic Structure of the Surface Complex. *J. Phys. Chem. C* **2014**, *118*, 2718–2725.

245. Gieseking, R. L.; Ratner, M. A.; Schatz, G. C. Theoretical Modeling of Voltage Effects and the Chemical Mechanism in Surface–Enhanced Raman Scattering. *Faraday Discuss.* **2017**, *205*, 149–171.

246. Valdivia, S.; Aranda, D.; Otero, J. C.; López-Tocón, I. Voltage Tuning of Photoinduced Charge Transfer Resonances between 2,2′-Bipyridine and a Nanostructured Silver Electrode. *Appl. Surf. Sci.* **2024**, *646*, 158871.

247. Aranda, D.; Valdivia, S.; Avila, F. J.; Soto, J.; Otero, J. C.; López-Tocón, I. Charge Transfer at the Nanoscale and the Role of the Out-of-Plane Vibrations in the Selection Rules of Surface-Enhanced Raman Scattering. *Phys. Chem. Chem. Phys.* **2018**, *20*, 29430–29439.

248. Gieseking, R. L. M.; Ratner, M. A.; Schatz, G. C. Benchmarking Semiempirical Methods To Compute Electrochemical Formal Potentials. *J. Phys. Chem. A* **2018**, *122*, 6809–6818.

249. Ding, S.-Y.; Liu, B.-J.; Jiang, Q.-N.; Wu, D.-Y.; Ren, B.; Xu, X.; Tian, Z.-Q. Cations-Modified Cluster Model for Density-Functional Theory Simulation of Potential Dependent Raman Scattering from Surface Complex/Electrode Systems. *Chem. Commun.* **2012**, *48*, 4962–4964.

250. Lopez-Ramirez, M. R.; Ruano, C.; Castro, J. L.; Arenas, J. F.; Soto, J.; Otero, J. C. Surface-Enhanced Raman Scattering of Benzoate Anion Adsorbed on Silver Nanoclusters: Evidence of the Transient Formation of the Radical Dianion. *J. Phys. Chem. C* **2010**, *114*, 7666–7672.

251. Arenas, J. F.; Woolley, M. S.; Otero, J. C.; Marcos, J. I. Charge-Transfer Processes in Surface-Enhanced Raman Scattering. Franck-Condon Active Vibrations of Pyrazine. *J. Phys. Chem.* **1996**, *100*, 3199–3206.

252. Hirakawa, A. Y.; Tsuboi, M. Molecular Geometry in an Excited Electronic State and a Preresonance Raman Effect. *science* **1975**, *188*, 359–361.

253. Podstawka, E.; Drąg, M.; Oleksyszyn, J. Raman and Surface-Enhanced Raman Studies

of α-Aminophosphinic Inhibitors of Metalloenzymes. *J. Raman Spectrosc.* **2009**, *40*, 1564–1571.

254. Kwasnieski, D. T.; Wang, H.; Schultz, Z. D. Alkyl-Nitrile Adlayers as Probes of Plasmonically Induced Electric Fields. *Chem. Sci.* **2015**, *6*, 4484–4494.

255. Shi, H.; Pekarek, R. T.; Chen, R.; Zhang, B.; Wang, Y.; Aravind, I.; Cai, Z.; Jensen, L.; Neale, N. R.; Cronin, S. B. Monitoring Local Electric Fields Using Stark Shifts on Napthyl Nitrile-Functionalized Silicon Photoelectrodes. *J. Phys. Chem. C* **2020**, *124*, 17000–17005.

256. Schkolnik, G.; Salewski, J.; Millo, D.; Zebger, I.; Franzen, S.; Hildebrandt, P. Vibrational Stark Effect of the Electric-Field Reporter 4-Mercaptobenzonitrile as a Tool for Investigating Electrostatics at Electrode/SAM/Solution Interfaces. *Int. J. Mol. Sci.* **2012**, *13*, 7466–7482.

257. Wilson, A. J.; Willets, K. A. Unforeseen Distance-Dependent SERS Spectroelectrochemistry from Surface-Tethered Nile Blue: The Role of Molecular Orientation. *Analyst* **2016**, *141*, 5144–5151.

258. Jiang, N.; Foley, E. T.; Klingsporn, J. M.; Sonntag, M. D.; Valley, N. A.; Dieringer, J. A.; Seideman, T.; Schatz, G. C.; Hersam, M. C.; Van Duyne, R. P. Observation of Multiple Vibrational Modes in Ultrahigh Vacuum Tip-Enhanced Raman Spectroscopy Combined with Molecular-Resolution Scanning Tunneling Microscopy. *Nano Lett.* **2012**, *12*, 5061–5067.

259. Alvarez-Puebla, R.; Liz-Marzan, L. M.; Garcia de Abajo, F. J. Light Concentration at the Nanometer Scale. *J. Phys. Chem. Lett.* **2010**, *1*, 2428–2434.

260. Barbry, M.; Koval, P.; Marchesin, F.; Esteban, R.; Borisov, A. G.; Aizpurua, J.; Sánchez-Portal, D. Atomistic Near-Field Nanoplasmonics: Reaching Atomic-Scale Resolution in Nanooptics. *Nano Lett.* **2015**, *15*, 3410–3419.

261. Lee, J.; Tallarida, N.; Chen, X.; Liu, P.; Jensen, L.; Apkarian, V. A. Tip-Enhanced Raman Spectromicroscopy of Co(II)-Tetraphenylporphyrin on Au(111): Toward the Chemists' Microscope. *ACS Nano* **2017**, *11*, 11466–11474.

262. Chiang, N.; Chen, X.; Goubert, G.; Chulhai, D. V.; Chen, X.; Pozzi, E. A.; Jiang, N.; Hersam, M. C.; Seideman, T.; Jensen, L.; Van Duyne, R. P. Conformational Contrast of Surface-Mediated Molecular Switches Yields Ångstrom-Scale Spatial Resolution in Ultrahigh Vacuum Tip-Enhanced Raman Spectroscopy. *Nano Lett.* **2016**, *16*, 7774–7778.

263. Jiang, S.; Zhang, Y.; Zhang, R.; Hu, C.; Liao, M.; Luo, Y.; Yang, J.; Dong, Z.; Hou, J. G. Distinguishing Adjacent Molecules on a Surface Using Plasmon-Enhanced Raman Scattering. *Nat. Nanotechnol.* **2015**, *10*, 865–869.

264. Shin, H.-H.; Yeon, G. J.; Choi, H.-K.; Park, S.-M.; Lee, K. S.; Kim, Z. H. Frequency-Domain Proof of the Existence of Atomic-Scale SERS Hot-Spots. *Nano Lett.* **2018**, *18*, 262–271.

265. Carnegie, C.; Griffiths, J.; de Nijs, B.; Readman, C.; Chikkaraddy, R.; Deacon, W. M.; Zhang, Y.; Szabb, I.; Rosta, E.; Aizpurua, J.; Baumberg, J. J. Room-Temperature Optical Picocavities below 1 nm^3 Accessing Single-Atom Geometries. *J. Phys. Chem. Lett.* **2018**, *9*, 7146–7151.

266. Kumar, N.; Su, W.; Veselý, M.; Weckhuysen, B. M.; Pollard, A. J.; Wain, A. J. Nanoscale Chemical Imaging of Solid-Liquid Interfaces Using Tip-Enhanced Raman Spectroscopy. *Nanoscale* **2018**, *10*, 1815–1824.

267. He, Z.; Han, Z.; Kizer, M.; Linhardt, R. J.; Wang, X.; Sinyukov, A. M.; Wang, J.; Deckert, V.; Sokolov, A. V.; Hu, J.; Scully, M. O. Tip-Enhanced Raman Imaging of Single-Stranded DNA with Single Base Resolution. *J. Am. Chem. Soc.* **2019**, *141*, 753–757.

268. Neacsu, C. C.; Dreyer, J.; Behr, N.; Raschke, M. B. Scanning-Probe Raman Spectroscopy with Single-Molecule Sensitivity. *Phys. Rev. B* **2006**, *73*, 193406.

269. Jiang, N.; Kurouski, D.; Pozzi, E. A.; Chiang, N.; Hersam, M. C.; Duyne, R. P. V. Tip-Enhanced Raman Spectroscopy: From Concepts to Practical Applications. *Chem. Phys. Lett.* **2016**, *659*, 16–24.

270. Tallarida, N.; Lee, J.; Apkarian, V. A. Tip-Enhanced Raman Spectromicroscopy on the Angstrom Scale: Bare and CO-Terminated Ag Tips. *ACS Nano* **2017**, *11*, 11393–11401.

271. Liu, P.; Chulhai, D. V.; Jensen, L. Single–Molecule Imaging Using Atomistic Near–Field Tip–Enhanced Raman Spectroscopy. *ACS Nano* **2017**, *11*, 5094–5102.

272. Zhang, Y.; Yang, B.; Ghafoor, A.; Zhang, Y.; Zhang, Y.-F.; Wang, R.-P.; Yang, J.-L.; Luo, Y.; Dong, Z.-C.; Hou, J. G. Visually Constructing the Chemical Structure of a Single Molecule by Scanning Raman Picoscopy. *Natl. Sci. Rev* **2019**, *6*, 1169–1175.

273. Fiederling, K.; Abasifard, M.; Richter, M.; Deckert, V.; Kupfer, S.; Gräfe, S. A Full Quantum Mechanical Approach Assessing the Chemical and Electromagnetic Effect in TERS. *ACS Nano* **2023**, *17*, 13137–13146.

274. Yang, B.; Chen, G.; Ghafoor, A.; Zhang, Y.-F.; Zhang, X.-B.; Li, H.; Dong, X.-R.; Wang, R.-P.; Zhang, Y.; Zhang, Y.; Dong, Z.-C. Chemical Enhancement and Quenching in Single-Molecule Tip-Enhanced Raman Spectroscopy. *Angew. Chem., Int. Ed.* **2023**, *62*, e202218799.

275. Duan, S.; Tian, G.; Ji, Y.; Shao, J.; Dong, Z.; Luo, Y. Theoretical Modeling of Plasmon-Enhanced Raman Images of a Single Molecule with Subnanometer Resolution. *J. Am. Chem. Soc.* **2015**, *137*, 9515–9518.

276. Latorre, F.; Kupfer, S.; Bocklitz, T.; Kinzel, D.; Trautmann, S.; Grafe, S.; Deckert, V.

Spatial Resolution of Tip-Enhanced Raman Spectroscopy - DFT Assessment of the Chemical Effect. *Nanoscale* **2016**, *8*, 10229–10239.

277. Fiederling, K.; Abasifard, M.; Richter, M.; Deckert, V.; Gräfe, S.; Kupfer, S. The Chemical Effect Goes Resonant – a Full Quantum Mechanical Approach on TERS. *Nanoscale* **2020**, *12*, 6346–6359.

278. Gieseking, R. L. M. Quantum Mechanical Effects in High-Resolution Tip-Enhanced Raman Imaging. *J. Phys. Chem. C* **2022**, *126*, 11690–11700.

279. Zuloaga, J.; Prodan, E.; Nordlander, P. Quantum Description of the Plasmon Resonances of a Nanoparticle Dimer. *Nano Lett.* **2009**, *9*, 887.

280. Teperik, T. V.; Nordlander, P.; Aizpurua, J.; Borisov, A. G. Quantum Effects and Nonlocality in Strongly Coupled Plasmonic Nanowire Dimers. *Opt. Express* **2013**, *21*, 27306–27325.

281. Zhu, W.; Crozier, K. B. Quantum Mechanical Limit to Plasmonic Enhancement as Observed by Surface-Enhanced Raman Scattering. *Nat. Commun.* **2014**, *5*, 5228.

282. Scholl, J. A.; García-Etxarri, A.; Koh, A. L.; Dionne, J. A. Observation of Quantum Tunneling between Two Plasmonic Nanoparticles. *Nano Lett.* **2013**, *13*, 564–569.

283. Savage, K. J.; Hawkeye, M. M.; Esteban, R.; Borisov, A. G.; Aizpurua, J.; Baumberg, J. J. Revealing the Quantum Regime in Tunnelling Plasmonics. *Nature* **2012**, *491*, 574–577.

284. Zhu, W.; Esteban, R.; Borisov, A. G.; Baumberg, J. J.; Nordlander, P.; Lezec, H. J.; Aizpurua, J.; Crozier, K. B. Quantum Mechanical Effects in Plasmonic Structures with Subnanometre Gaps. *Nat. Commun.* **2016**, *7*, 11495.

285. Esteban, R.; Borisov, A. G.; Nordlander, P.; Aizpurua, J. Bridging Quantum and Classical Plasmonics with a Quantum-Corrected Model. *Nat. Commun.* **2012**, *3*, 825.

286. Kravtsov, V.; Berweger, S.; Atkin, J. M.; Raschke, M. B. Control of Plasmon Emission and Dynamics at the Transition from Classical to Quantum Coupling. *Nano Lett.* **2014**, *14*, 5270–5275.

287. Lin, L.; Zhang, Q.; Li, X.; Qiu, M.; Jiang, X.; Jin, W.; Gu, H.; Lei, D. Y.; Ye, J. Electron Transport Across Plasmonic Molecular Nanogaps Interrogated with Surface-Enhanced Raman Scattering. *ACS Nano* **2018**, *12*, 6492–6503.

288. Liu, S.; Cirera, B.; Sun, Y.; Hamada, I.; Müller, M.; Hammud, A.; Wolf, M.; Kumagai, T. Dramatic Enhancement of Tip-Enhanced Raman Scattering Mediated by Atomic Point Contact Formation. *Nano Lett.* **2020**, *20*, 5879–5884.

289. Liu, S.; Hammud, A.; Wolf, M.; Kumagai, T. Atomic Point Contact Raman Spectroscopy of a Si(111)-7 $\times$ 7 Surface. *Nano Lett.* **2021**, *21*, 4057–4061.

290. Cirera, B.; Litman, Y.; Lin, C.; Akkoush, A.; Hammud, A.; Wolf, M.; Rossi, M.; Kumagai, T. Charge Transfer-Mediated Dramatic Enhancement of Raman Scattering upon Molecular Point Contact Formation. *Nano Lett.* **2022**, *22*, 2170–2176.

291. Pérez-González, O.; Zabala, N.; Borisov, A. G.; Halas, N. J.; Nordlander, P.; Aizpurua, J. Optical Spectroscopy of Conductive Junctions in Plasmonic Cavities. *Nano Lett.* **2010**, *10*, 3090–3095.

292. Liu, P.; Chulhai, D. V.; Jensen, L. Atomistic Characterization of Plasmonic Dimers in the Quantum Size Regime. *J. Phys. Chem. C* **2019**, *123*, 13900–13907.

293. Urbieta, M.; Barbry, M.; Zhang, Y.; Koval, P.; Sánchez-Portal, D.; Zabala, N.; Aizpurua, J. Atomic-Scale Lightning Rod Effect in Plasmonic Picocavities: A Classical View to a Quantum Effect. *ACS Nano* **2018**, *12*, 585–595.

294. Litman, Y.; Bonafé, F. P.; Akkoush, A.; Appel, H.; Rossi, M. First-Principles Simu-

lations of Tip Enhanced Raman Scattering Reveal Active Role of Substrate on High-Resolution Images. *J. Phys. Chem. Lett.* **2023**, *14*, 6850–6859.

295. Thiel, W. Semiempirical Quantum–Chemical Methods. *WIREs Comput. Mol. Sci.* **2014**, *4*, 145–157.

296. Bannwarth, C.; Caldeweyher, E.; Ehlert, S.; Hansen, A.; Pracht, P.; Seibert, J.; Spicher, S.; Grimme, S. Extended Tight-Binding Quantum Chemistry Methods. *WIREs Comput. Mol. Sci.* **2021**, *11*, e1493.

297. Jacob, C. R.; Neugebauer, J. Subsystem Density-Functional Theory (Update). *WIREs Comput. Mol. Sci.* **2024**, *14*, e1700.

298. Sun, Q.; Chan, G. K.-L. Quantum Embedding Theories. *Acc. Chem. Res.* **2016**, *49*, 2705–2712.

299. Gomes, A. S. P.; Jacob, C. R. Quantum-Chemical Embedding Methods for Treating Local Electronic Excitations in Complex Chemical Systems. *Annu. Rep. Prog. Chem., Sect. C: Phys. Chem.* **2012**, *108*, 222–277.

300. Deringer, V. L.; Bartók, A. P.; Bernstein, N.; Wilkins, D. M.; Ceriotti, M.; Csányi, G. Gaussian Process Regression for Materials and Molecules. *Chem. Rev.* **2021**, *121*, 10073–10141.

301. Keith, J. A.; Vassilev-Galindo, V.; Cheng, B.; Chmiela, S.; Gastegger, M.; Müller, K.-R.; Tkatchenko, A. Combining Machine Learning and Computational Chemistry for Predictive Insights Into Chemical Systems. *Chem. Rev.* **2021**, *121*, 9816–9872.

302. Dral, P. O. Quantum Chemistry in the Age of Machine Learning. *J. Phys. Chem. Lett.* **2020**, *11*, 2336–2347.

TOC Graphic